
Reasoning is Periodicity? Improving Large Language Models Through Effective Periodicity Modeling

Yihong Dong¹, Ge Li^{1,2}, Xue Jiang¹, Yongding Tao¹, Kechi Zhang¹, Hao Zhu¹, Huanyu Liu¹,
Jiazheng Ding², Jia Li ^σ¹, Jinliang Deng³, and Hong Mei^{1,4}

¹School of Computer Science, Peking University ²aiXcoder

³The Hong Kong University of Science and Technology ⁴Advanced Institute of Big Data
dongyh@stu.pku.edu.cn, lige@pku.edu.cn

Abstract

Periodicity, as one of the most important basic characteristics, lays the foundation for facilitating structured knowledge acquisition and systematic cognitive processes within human learning paradigms. However, the potential flaws of periodicity modeling in Transformer affect the learning efficiency and establishment of underlying principles from data for large language models (LLMs) built upon it. In this paper, we demonstrate that integrating effective periodicity modeling can improve the learning efficiency and performance of LLMs. We introduce FANformer, which adapts Fourier Analysis Network (FAN) into attention mechanism to achieve efficient periodicity modeling, by modifying the feature projection process of attention mechanism. Extensive experimental results on language modeling show that FANformer consistently outperforms Transformer when scaling up model size and training tokens, underscoring its superior learning efficiency. Our pretrained FANformer-1B exhibits marked improvements on downstream tasks compared to open-source LLMs with similar model parameters or training tokens. Moreover, we reveal that FANformer exhibits superior ability to learn and apply rules for reasoning compared to Transformer. The results position FANformer as an effective and promising architecture for advancing LLMs. Our code is available at <https://github.com/YihongDong/FANformer..>

1 Introduction

In recent years, large language models (LLMs) have achieved remarkable progress across various natural language processing tasks, establishing themselves as a cornerstone of modern artificial intelligence [Brown et al., 2020, Zhao et al., 2023, Minaee et al., 2024]. The decoder-only Transformer architecture, in particular, has emerged as the de facto standard for LLM development due to its superior performance and scalability [OpenAI, 2023, DeepSeek-AI et al., 2024a, Groeneveld et al., 2024]. Besides these advancements, Transformer-based models are also known for their immense demand for data and computational resources during training [Kaplan et al., 2020, Hoffmann et al., 2022, Chowdhery et al., 2023]. In comparison, humans are able to accomplish similar learning tasks with far fewer resources. This discrepancy suggests that existing LLM architectures still suffer from low learning efficiency, leaving substantial room for improvement in their ability to extract and generalize the knowledge from data.

Periodicity, characterized by recurring patterns, is a ubiquitous phenomenon in human life and learning processes [Buzsaki, 2006, Lake et al., 2017]. The human brain leverages pattern recognition mechanisms to process information and acquire knowledge efficiently [Zalta et al., 2020, Edalati et al., 2023, Zhan et al., 2018]. However, general network architectures represented by Transformers have potential flaws in periodicity modeling, which could hinder their learning efficiency [Dong et al.,

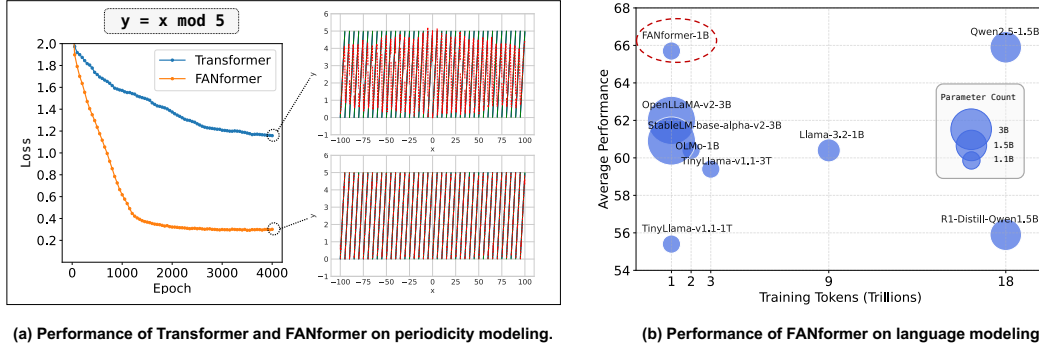


Figure 1: The performance of FANformer on periodicity modeling and language modeling. (a) shows the training loss of Transformer and FANformer on the fitting mod function and their performance at the 4,000th epoch. (b) shows the average performance of 8 core commonsense tasks between FANformer-1B and the open-source LLMs with comparable model parameters and training tokens.

2024a, Liu et al., 2020]. As shown in Figure 1 (a), even for a simple mod function, Transformer demonstrates suboptimal performance despite being provided with sufficient training data and model capacity¹. This inefficiency can be exacerbated during the training process of LLMs to affect their performance, considering the periodicity hidden in large amounts of language data. Fourier Analysis Network (FAN) [Dong et al., 2024a] has shown preliminary success in tasks with explicit or implicit periodic features, but its adaptation to Transformer architectures for large-scale language modeling remains an open challenge.

In this paper, we present FANformer, a novel foundation architecture for LLMs that adapts FAN into the attention mechanism of Transformer to improve learning efficiency and model performance through effective periodicity modeling. It leverages FAN to introduce Fourier principles for capturing and representing periodic patterns, thereby enhancing the Transformer’s capability to learn and generalize from data. Specifically, we modify the feature projection process of attention mechanism to incorporate frequency-domain representations to facilitate modeling periodicity. Figure 1 (a) demonstrates the significant advantages of FANformer over Transformer on periodicity modeling, with faster convergence speed and better results. In Figure 1 (b), we can observe that FANformer-1B achieves superior performance with higher utilization efficiency of model parameters and training tokens when benchmarked against comparable Transformer-based LLMs.

To comprehensively validate the effectiveness and scalability of FANformer, we conduct extensive experiments on language modeling tasks. The results of scaling both model parameters and training tokens highlight that FANformer consistently surpasses Transformer, requiring only 69.2% of model parameters or 79.7% of training tokens to achieve comparable performance. We also implement a complete pretraining pipeline to pretrain a 1.1-billion parameter FANformer (FANformer-1B) on 1 trillion tokens. Experiments on various downstream tasks demonstrate that FANformer-1B outperforms open-source LLMs of the same size with fewer training tokens, and exceeds LLMs with three times the parameters when using the same training token. Through further analysis, we reveal that FANformer is a superior choice compared to other variant architectures and discover three interesting findings: 1) By observing the training process, we discover the notable enhancements in FANformer’s learning efficiency over Transformer as the model continues to learn from the data. 2) FANformer facilitates the rule-based reasoning paradigm, mitigating the occurrence of "holes" inherent in the case-based learning of Transformer [Hu et al., 2024]. Under the stress test of logical reasoning [Wang et al., 2024], FANformer-1B demonstrates superior performance compared to OLMo-1B and Qwen2.5-1.5B. 3) FANformer’s representational capacity consistently surpasses that of Transformer across various layer depths, as evidenced by evaluations of the model’s Lipschitz constant [Latorre et al., 2020]. These findings underscore the potential of FANformer as an effective and scalable architecture for advancing LLMs.

The main contributions of our work can be summarized as three points: **1** We first demonstrate that integrating effective periodicity modeling can improve the learning efficiency and performance of

¹We sample 400K training data from the function of mod 5 and train a 110M Transformer for 4K epochs.

LLMs. ② We propose FANformer, a novel LLM architecture, which uses a simple yet effective approach to adapt FAN into attention mechanism for efficient periodicity modeling, consistently outperforming Transformers in scaling model parameters and training tokens. ③ We pretrain and open-source FANformer-1B, which surpasses SOTA publicly available LLMs with similar parameter counts or training token budgets on downstream tasks.

2 Motivation

In this section, we combine formalization with illustrative cases to demonstrate why periodicity modeling facilitates language modeling and reasoning, thereby elucidating the motivation behind the development of FANformer.

The essence of periodicity lies in the repetitive manifestation of certain invariance under transformations, which can be strictly defined through invariance under group actions in Abstract Algebra Dummit and Foote [2004]. Let X be a set and G be a group acting on X . An element $x \in X$ is said to be periodic with respect to the action of G if there exists a non-identity element $p \in G$ such that $p \cdot x = x$, where \cdot denotes the group action. The element p is called a period of x . Periodicity implies that x is invariant under the action of the cyclic subgroup generated by p , denoted by $\langle p \rangle$. For example, $f(a) = f(a + T)$ can be seen as a specific instance of the abstract definition $p \cdot x = x$, where $x = f$, $p = T$, and the group action is translation. When the input a and the group G are extended to higher dimensions or non-temporal domains, the manifestation of the period T also changes accordingly. Crucially, for many reasoning tasks, the underlying operation or inference rule remains invariant across structurally similar subproblems, that is, for all inputs belonging to a certain equivalence class, the same functional rule is applied, which precisely reflects periodic invariance.

Consider addition as an illustrative case: let f represent the addition operation, a denote the digit position index, and let the period $T = 1$ correspond to the positional shift in place value. The reasoning proceeds as:

Example: $357 + 286 = ?$
Digit-wise operations: units ($7 + 6 = 13 \rightarrow$ write 3, carry 1); tens ($5 + 8 + 1 = 14 \rightarrow$ write 4, carry 1); hundreds ($3 + 2 + 1 = 6 \rightarrow$ write 6).
Result: 643

Thus, the periodicity of addition is manifested in the repeated application of the same rule across different digit positions, where the rule itself remains invariant under positional shifts. It can be extended to other reasoning, such as logical reasoning, and the scenario is analogous: when a neural network extracts a feature applicable to specific conditions or premises, it repeatedly applies the same invariant rules across analogous subproblems. Such periodic invariance allows for enhancing both the learning efficiency and generalization capability of neural models by reducing redundancy and reinforcing conceptual regularities.

3 FANformer

We will provide a detailed description of FANformer for sequence modeling and adopt a decoder-only model to illustrate the architecture.

Given an input sequence $s = \{s_1, s_2, \dots, s_l\}$, where s_i denotes the i -th token and l represents the length of sequence s , it is first mapped to the input embedding as $\mathbf{X}^0 = [\mathbf{x}_1, \mathbf{x}_2, \dots, \mathbf{x}_l] \in \mathbb{R}^{l \times d_h}$, where d_h represents the model’s hidden dimension. The embedding is subsequently fed into the model to obtain the final output \mathbf{X}^N , with each n -th layer of FANformer processing \mathbf{X}^{n-1} , where $n \in [1, N]$. The core of each FANformer layer lies in a revised attention module that incorporates a modified FAN layer, referred to as the ATtention-Fourier (ATF) module.

3.1 ATF

The attention mechanism serves as a core component of Transformer architectures, enabling dynamic interaction between tokens through query-key-value (QKV) projections. While effective for general sequence modeling, its standard implementation exhibits limitations in capturing periodic patterns due to the inherent locality of linear projections in the time domain. To address this, we propose

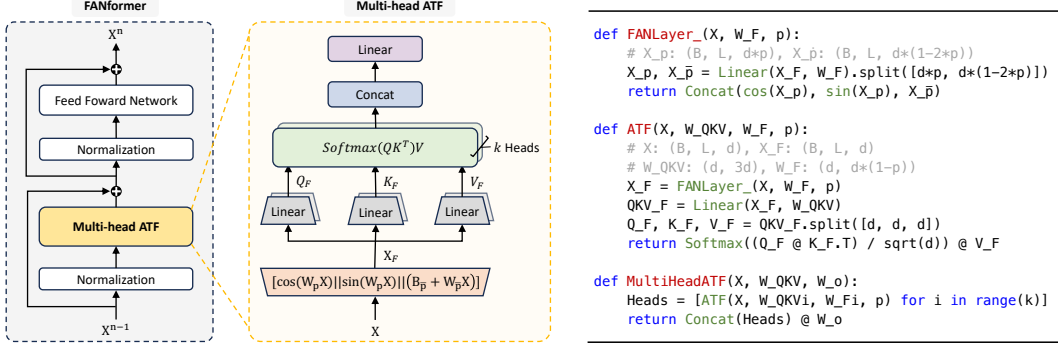


Figure 2: Left: The illustration of FANformer’s architecture. Right: The pseudocode of Multi-head ATF, where p is the hyperparameter that controls the proportion of periodicity modeling for X_p .

the ATF module, which incorporates the operations of FAN into the QKV projection process to explicitly model periodicity in the frequency domain. Specifically, given the input $\mathbf{X} \in \mathbb{R}^{l \times d_h}$, we first calculate $\mathbf{X}_F \in \mathbb{R}^{l \times d_h}$ as:

$$\mathbf{X}_F = \text{FANLayer}'(\mathbf{X}) = [\cos(W_p \mathbf{X}) \parallel \sin(W_p \mathbf{X}) \parallel (W_{\bar{p}} \mathbf{X} + B_{\bar{p}})], \quad (1)$$

where $\text{FANLayer}'$ represents a variant of the original FAN layer (i.e., Eq. (10)) with the activation function σ in Eq. (10) replaced by the identity function, i.e., $\sigma(x) = x$, in this paper, and hyperparameter p is defined as the proportion of $\frac{d_{W_p}}{d_h}$. On this basis, we employ the linear transform to \mathbf{X}_F to compute QKV projections, i.e., $\mathbf{Q}_F, \mathbf{K}_F, \mathbf{V}_F \in \mathbb{R}^{l \times d_h}$, as follows:

$$[\mathbf{Q}_F, \mathbf{K}_F, \mathbf{V}_F] = \mathbf{X}_F [\mathbf{W}_Q, \mathbf{W}_K, \mathbf{W}_V], \quad (2)$$

where $\mathbf{W}_Q, \mathbf{W}_K, \mathbf{W}_V \in \mathbb{R}^{d_h \times d_h}$ are learnable parameters. Similar to the standard attention mechanism, the computation of ATF is defined as:

$$\text{ATF}(\mathbf{X} | \mathbf{W}_Q, \mathbf{W}_K, \mathbf{W}_V) = \text{softmax} \left(\frac{\mathbf{Q}_F \mathbf{K}_F^T}{\sqrt{d_h}} \right) \mathbf{V}_F, \quad (3)$$

where $\mathbf{Q}_F, \mathbf{K}_F, \mathbf{V}_F$ are computed using the input \mathbf{X} via Eq. (1) and Eq. (2). To enhance the model’s capacity, we extend the ATF module to multiple heads. Given input $\mathbf{X} \in \mathbb{R}^{l \times d_h}$, the Multi-head ATF first projects \mathbf{X} into k independent heads through the ATF module. For the i -th head, we have:

$$\text{Head}_i = \text{ATF}(\mathbf{X} | \mathbf{W}_Q^i, \mathbf{W}_K^i, \mathbf{W}_V^i), \quad (4)$$

where $\mathbf{W}_Q^i, \mathbf{W}_K^i, \mathbf{W}_V^i \in \mathbb{R}^{d_h \times d_k}$ are learnable parameters for query, key, and value projections respectively, with $d_k = d_h/k$. The outputs of all heads are concatenated and linearly transformed:

$$\text{MultiHeadATF}(\mathbf{X}) = [\text{Head}_1 \parallel \dots \parallel \text{Head}_k] \mathbf{W}_O, \quad (5)$$

where $\mathbf{W}_O \in \mathbb{R}^{d_h \times d_h}$ is the learnable parameter of out projection matrix. Note that $\text{ATF}(\mathbf{X})$ is mathematically equivalent to $\text{Attention}(\text{FANLayer}'(\mathbf{X}))$ (the detailed derivations are provided in Appendix L). This equivalence enables a simple yet effective implementation of Multi-head ATF as shown in Figure 2, which can seamlessly incorporate various advancements in traditional attention mechanisms, such as FlashAttention [Dao et al., 2022].

3.2 Overall Architecture

The FANformer model comprises N stacked FANformer layers, where each FANformer layer consists of a Multi-head ATF module and a feed-forward network (FFN) module. Following the previous work [Groeneveld et al., 2024, Touvron et al., 2023a], we employ SwiGLU [Ramachandran et al., 2018, Shazeer, 2020] and pre-norm [Zhang and Sennrich, 2019] as the enhancements to Transformer-based LLMs. Specifically, the n -th FANformer layer can be defined as:

$$\mathbf{Y}^n = \text{MultiHeadATF}(\text{Norm}(\mathbf{X}^n)) + \mathbf{X}^n, \quad (6)$$

$$\mathbf{X}^{n+1} = \text{FFN}(\text{Norm}(\mathbf{Y}^n)) + \mathbf{Y}^n, \quad (7)$$

where the MultiHeadATF module is computed via Eq. (5) and the FFN module, which leverages the SwiGLU activation, is expressed as:

$$\text{FFN}(\mathbf{X}) = (\text{Swish}(\mathbf{X}\mathbf{W}_1) \otimes \mathbf{X}\mathbf{W}_2)\mathbf{W}_3, \quad (8)$$

where $\mathbf{W}_1, \mathbf{W}_2 \in \mathbb{R}^{d_n \times d_f}$, $\mathbf{W}_3 \in \mathbb{R}^{d_f \times d_n}$ are learnable parameters, \otimes denotes element-wise multiplication, and d_f is the intermediate dimension. The overview of FANformer’s architecture is illustrated in Figure 2.

4 Evaluation

We begin with the implementation details of our experiments (Section 4.1), followed by a comprehensive evaluation of FANformer from three distinct perspectives: First, we investigate the scalability of FANformer by examining its performance trends on language modeling tasks with respect to model size and training tokens (Section 4.2). Second, we evaluate the capabilities of the pre-trained FANformer-1B model across multiple downstream tasks (Section 4.3). Third, we conduct an in-depth empirical analysis of FANformer, including ablation study, learning efficiency, reasoning mechanism, representational capacity, and more (Section 4.4). See Appendix A-J for more experiments.

4.1 Implementation Details

The experiments are conducted on 80 A100 GPUs. We build FANformer upon the foundation of OLMo [Groeneveld et al., 2024], as it provides a solid pretraining framework of LLMs, with the hyperparameter p set to 0.25 by default. For pretraining FANformer-1B, we randomly sample 1T training tokens from OLMo’s training data, i.e., Dolma [Soldaini et al., 2024]. For other experiments, we train models on a smaller sample of Dolma, i.e., Dolma v1_6-sample [AllenAI, 2023], with roughly 10B tokens. The detailed pretraining and experimental setups are provided in Appendix M.

4.2 Scalability of FANformer

We explore the scalability of FANformer compared with Transformer to investigate performance trends in the construction of much larger models.

Setup. We follow OLMo’s configuration and vary the FFN’s intermediate dimension d_f to keep the number of parameters consistent for all models in this experiment. For scaling up model parameters, we adopt Dolma v1_6-sample as training data and train LLMs from 268M to 7B. We compare FANformer with the standard Transformer and a variant of FANformer, termed Transformer+ATM, which uses MLP layer instead of FAN layer in FANformer. For scaling up training tokens, we train 1B LLMs on the first 200 billion of our sampled 1T tokens.

Results. As shown in Figure 3, the scaling law [Kaplan et al., 2020] empirically aligns well with the results obtained from our FANformer, underscoring its superior scalability properties. Figure 3 (left) reveals that the implementation of FAN consistently surpasses the performance of the standard Transformer across a range of model sizes. This finding highlights FANformer’s enhanced scalability in terms of parameter efficiency, as it achieves comparable performance with only 69.2% of the parameters required by the standard Transformer. Notably, the scaling curve of Transformer+ATM closely overlaps with that of the standard Transformer, indicating that merely revising attention mechanisms using MLP Layer is insufficient. This observation further emphasizes that FANformer’s performance gains are not attributable to network depth increase, but rather to its special architectural design. Figure 3 (right) demonstrates that FANformer achieves performance parity with the standard Transformer while utilizing significantly fewer training tokens. Specifically, FANformer requires only 159.6B training

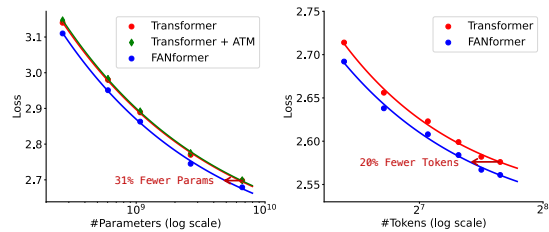


Figure 3: Language modeling loss of scaling up model parameters and training tokens. Left: we train LLMs from 268M to 7B parameters. Right: we evaluate LLMs every 20B tokens up to 200B tokens.

Table 1: Zero-shot performance of FANformer-1B versus other comparable open-source LLMs on 8 core tasks from the downstream evaluation suite following OLMo. The results of baselines are taken from the previous works [Groeneveld et al., 2024, Ye et al., 2024, Dong et al., 2024b].

Models	Param.	Tokens	ARC-C	ARC-E	BoolQ	Hella.	OBQA	PIQA	SCIQ	Wino.	Avg.
LLMs around 1B parameters											
Qwen2.5-1.5B	1.5B	18T	41.2	75.5	74.0	50.2	52.4	75.7	94.7	63.3	65.9
R1-Distill-Qwen1.5B	1.5B	18T+	36.2	54.4	69.1	41.8	35.4	65.1	89.5	55.3	55.9
Llama-3.2-1B	1.1B	9T	31.4	65.6	64.3	47.8	46	74.5	92.3	60.7	60.4
TinyLlama-v1.1 (3T)	1.1B	3T	34.8	53.2	64.6	58.7	43.6	71.1	90.5	58.9	59.4
OLMo-1B	1.1B	2T	34.5	58.1	60.7	62.5	46.4	73.7	88.1	58.9	60.4
LLMs trained on 1T tokens											
OpenLLaMA-v2-3B	3B	1T	33.9	67.6	65.7	70.0	26	76.7	92.9	62.9	62.0
StableLM-v2-3B	3B	1T	32.4	67.3	64.6	68.6	26.4	76	89.5	62.1	60.9
TinyLlama-v1.1 (1T)	1.1B	1T	33.1	49.5	58.4	52.5	37.8	70.4	86.4	55.2	55.4
FANformer-1B	1.1B	1T	43.8	72.5	64.9	64.7	48.2	75.5	94.8	61.3	65.6

tokens to match the performance of the standard Transformer trained on 200B tokens, representing a 20.3% reduction in training resource requirements. These findings suggest that FANformer exhibits superior utilization efficiency in terms of both model parameters and training tokens compared to the standard Transformer architecture.

4.3 Performance of FANformer-1B

We pretrain FANformer-1B on 1 trillion tokens and report zero-shot performance on a set of commonsense downstream tasks, following previous work [Brown et al., 2020, Touvron et al., 2023b, Groeneveld et al., 2024, inter alia].

Setup. The downstream evaluation suite consists of 8 core commonsense tasks, including ARC-C [Clark et al., 2018], ARC-E [Clark et al., 2018], BoolQ [Clark et al., 2019], HellaSwag [Zellers et al., 2019], OBQA [Mihaylov et al., 2018], PIQA [Bisk et al., 2020], SCIQ [Welbl et al., 2017], and WinoGrande [Sakaguchi et al., 2020]. We compare pretrained FANformer-1B to seven open-source LLMs with comparable model parameters or training tokens, including Qwen2.5-1.5B [Team, 2024], R1-Distill-Qwen1.5B [DeepSeek-AI et al., 2025], Llama-3.2-1B [Dubey et al., 2024], TinyLlama-v1.1-1B [Zhang et al., 2024], OLMo-1B [Groeneveld et al., 2024], OpenLLaMA-v2-3B [Geng and Liu, 2023], and StableLM-v2-3B [Tow, 2023].

Results. Table 1 presents the evaluation results of our pre-trained FANformer-1B on downstream tasks. It is evident that FANformer-1B surpasses LLMs with comparable parameter sizes, such as Llama-3.2-1B, TinyLlama-v1.1-3T, and OLMo-1B, while utilizing significantly fewer training data. Compared to the base model OLMo-1B, FANformer-1B achieves a relative improvement of 8.8% in the average performance of downstream tasks using only half the training data. On these tasks, FANformer-1B also demonstrates performance comparable to Qwen2.5-1.5B, which is the current SOTA LLM around 1B. For LLMs training on 1T tokens, FANformer-1B even exceeds LLMs with three times the parameters, showing an average relative performance improvement of 6.0-7.9% across all tasks. Moreover, while R1-Distill-Qwen1.5B shows notable improvements in reasoning capabilities based on its reported performance, it exhibits significantly weaker general performance on these commonsense downstream tasks. This observation shows the shortcomings of distillation, highlighting the necessity of the pre-training stage and the importance of research into more efficient model architectures.

4.4 Further Analysis

4.4.1 Ablation Study and Variant Analysis

Setup. We compare FANformer to other variant architectures, including 1) the above-mentioned Transformer+ATM, 2) Transformer+ATL, which use two linear transforms to compute QKV projection, 3) FANformer (original FAN) that employs Eq. (10) (original FAN layer) instead of Eq. (1) in FANformer, 4) Transformer (FFN \leftarrow FAN) where the FFN is replaced with FAN [Dong et al., 2024a], and 5) standard Transformer as their ablations.

Table 2: Results of ablation study and variant analysis on LLMs with 1B parameters trained on Dolma v1_6-sample dataset (about 10B tokens). The complete experimental results can be found in Table 8 and Table 9 of Appendix.

Variants	Param.	Training Loss ↓	V2 Eval Loss ↓	V2 Eval PPL ↓	V3 Eval Loss ↓	V3 Eval PPL ↓	DownStream Avg Acc. ↑
Transformer	1.0×	2.889	3.33	30.20	3.07	24.28	53.10
Transformer (FFN ← FAN)	1.0×	2.880	3.31	29.79	3.05	23.96	53.95
Same Parameter							
Transformer + ATM	1.0×	2.890	3.33	30.31	3.07	24.36	53.69
Transformer + ATL	1.0×	2.882	3.31	29.68	3.05	23.97	53.46
FANformer (original FAN)	1.0×	2.893	3.34	30.64	3.07	24.50	53.61
FANformer	1.0×	2.863	3.30	29.40	3.04	23.62	55.19
Same Dimension							
Transformer + ATM	1.06×	2.886	3.33	30.18	3.06	24.28	52.86
Transformer + ATL	1.06×	2.879	3.31	29.76	3.05	23.94	54.23
FANformer (original FAN)	1.04×	2.887	3.34	30.57	3.07	24.39	53.13
FANformer	1.04×	2.856	3.29	29.22	3.03	23.47	54.88

Results. From Table 2, we have the following findings: 1) FANformer consistently outperforms other variant architectures in both scenarios of the same parameter and same dimension on all evaluation metrics. 2) The performance of Transformer+ATM and Transformer+ATL is notably inferior to that of FANformer, indicating that the core improvement stems from the ATF module we designed. 3) Although Transformer (FFN ← FAN) yields some improvement, this enhancement is inferior to the gains achieved by FANformer, suggesting that integrating periodicity modeling within attention is more advantageous than FFN on language modeling. 4) Incorporating activation functions such as GELU into the attention mechanism tends to degrade model performance. Specifically, FANformer (original FAN) and Transformer+ATM exhibit weaker performance compared to FANformer and Transformer+ATL, likely because these activation functions suppress certain features, thereby hindering subsequent attention operations.

4.4.2 Training Dynamics

We perform a comparative analysis of the loss trends during the training process between our FANformer and Transformer, as illustrated in Figure 4. The experimental results indicate that the loss of FANformer decreases more slowly in the early stages compared to Transformer, which we hypothesize may be due to the initial lack of established periodic modeling. As the training progresses and periodic modeling gradually improves, FANformer demonstrates a faster convergence rate, with its loss decreasing more rapidly than that of Transformer. Intuitively, once the core of semantic knowledge is established, the model’s inherent periodic modeling lets new concepts attach to existing representations instead of being learned from scratch, accelerating subsequent learning. This result suggests that as the model progressively learns from the data, the learning efficiency of our FANformer notably surpasses the standard Transformer.

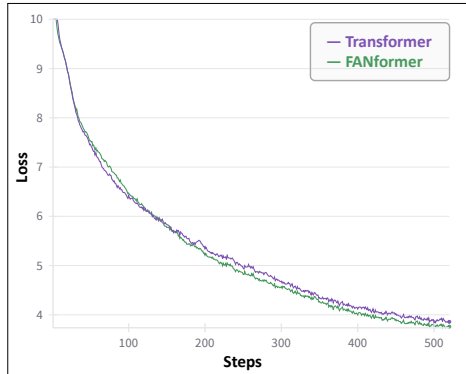


Figure 4: Training loss of FANformer and Transformer on early training steps, with the complete training loss is provided in Figure 7 of Appendix.

4.4.3 Case-based and Rule-based Reasoning

Setup. Following the work [Hu et al., 2024], we evaluate the case-based and rule-based reasoning of Transformer and our FANformer on two tasks, including: (1) Modular addition: $c = (a + b) \bmod 113$ with $a, b \in [0, 112]$; (2) Linear regression: $c = a + 2b + 3$ with $a, b \in [0, 99]$. We finetune pretrained LLMs, i.e., OLMo-1B and FANformer-1B, on each task dataset for 500 epochs and their performance is measured via the Leave-Square-Out method (10 samples per test point).

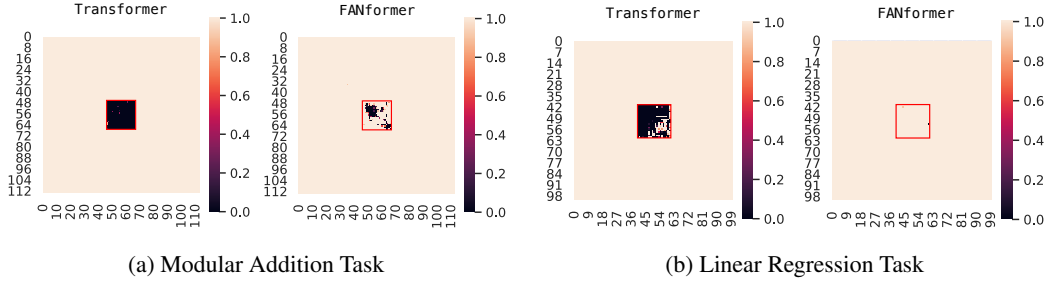


Figure 5: Performance of FANformer and Transformer on modular addition and linear regression tasks, where the darkened regions indicate areas where the model performance approaches zero, signifying the emergence of the "hole" as described in the work [Hu et al., 2024].

Results. As shown in Figure 10 of Appendix, both Transformer and our FANformer achieve near-perfect accuracy on the training set of modular addition and linear regression tasks, approaching approximately 100%. However, a critical divergence emerges in their performance on the test sets. Specifically, as shown in Figure 5, Transformer exhibits a pronounced failure to generalize, resulting in a "black hole" in the center of the figure, indicating that its accuracy on the test dataset drops to nearly zero. This observation is consistent with the findings reported in the work [Hu et al., 2024]. In contrast, FANformer demonstrates a marked improvement in addressing the "hole" issue. In the linear regression and modular addition tasks, there is no obvious hole observed, further corroborating the hypothesis that, relative to the Transformer-based model, FANformer possesses a stronger tendency to learn underlying rules, thereby achieving superior generalization performance.

4.4.4 LLMs' Proficiency in Logical Reasoning

Setup. Following the work [Wang et al., 2024], we adopt the ULogic dataset to systematically evaluate LLMs on their ability to capture underlying inferential logic, where ULogic is constructed after these LLM's training data cutoff, which prevents data contamination [Dong et al., 2024c]. We leverage the Law of Non-Contradiction [Priest et al., 2006], each rule is paired with a negated-conclusion variant; a response is correct only if the model accepts the original and rejects its flip. We evaluate FANformer-1B, OLMo-1B, Qwen2.5-1.5B, and GPT-4 on the two most challenging levels of ULogic for stress-testing.

Results. Table 3 summarizes the results on ULogic dataset, with an illustrative case presented in Figure 13 of Appendix. FANformer-1B substantially outperforms both Qwen2.5-1.5B and OLMo-1B: OLMo-1B naively labels every rule as True, and Qwen2.5-1.5B yields largely contradictory answers, whereas FANformer-1B can affirm the original rule and reject its negated counterpart. These results highlight FANformer's superiority in logic reasoning and underscore the architectural advantages conferred by the periodicity-aware design of FANformer.

Table 3: Average performance of different LLMs on ULogic.

Model	Acc (%)
GPT-4	65.1
OLMo-1B	0.0
Qwen2.5-1.5B	7.1
FANformer-1B	38.2

4.4.5 Representational Capacity

Setup. We explain the advantage of FANformer architecture from another perspective: the model's ability to learn complex functions. A larger Lipschitz constant L is frequently linked to greater representational capacity [Latorre et al., 2020, Bartlett et al., 2017], as it enables neural networks to approximate more intricate functional mappings by loosening smoothness constraints in parameter space. This relationship stems from the theoretical framework where less restrictive Lipschitz

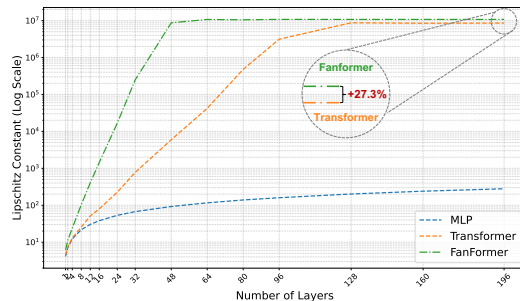


Figure 6: Representational capacity of MLP, Transformer, and FANformer across various layer depths.

conditions permit sharper decision boundaries and richer expressive power. Formally, L satisfies:

$$\forall x, y \in \mathbb{R}^n, \quad \|f_{\text{model}}(x) - f_{\text{model}}(y)\| \leq L\|x - y\|. \quad (9)$$

Results. We evaluate the representational capacity of MLP, Transformer, and FANformer across various layer depths via computing their Lipschitz constant L . Although representational capacity rises for all three architectures as additional layers are stacked, the growth rates diverge substantially. FANformer exhibits the steepest trajectory and attains the largest Lipschitz constant L at each depth, consistently surpassing Transformer by 27.3% in deeper configurations. These findings indicate that FANformer has markedly richer expressiveness and a superior ability to model complex functions.

5 Related Work

Large Language Models The rapid advancement of LLMs has revolutionized NLP and AI research [Radford, 2018, Dubey et al., 2024, DeepSeek-AI et al., 2025]. The emergence of GPT-3 [Brown et al., 2020], with 175B parameters, showcased remarkable few-shot prompting abilities, suggesting that scaling laws [Kaplan et al., 2020] could unlock emergent capabilities. Recent notable LLMs like PaLM [Chowdhery et al., 2023], LLaMA [Touvron et al., 2023b], GPT-4 [Chowdhery et al., 2023], and DeepSeek [Bi et al., 2024] further pushed the boundaries of model size and performance. Moreover, the open-source release of OLMo [Groeneveld et al., 2024] has provided valuable resources for the community, enabling more accessible training of LLMs.

Advances in Transformer Architecture Recent advancements in Transformer architecture focus on overcoming two main limitations: computational inefficiency in long-context processing and limited expressiveness of attention mechanisms. To address long-context inefficiencies, techniques such as sparsity [Child et al., 2019] and local attention [Beltagy et al., 2020], along with innovations in query mechanisms [Shazeer, 2019, Ainslie et al., 2023] and inference acceleration [DeepSeek-AI et al., 2024b], have been proposed. Hardware-level optimizations like FlashAttention [Dao et al., 2022] further reduce GPU memory access overhead. To enhance the expressiveness of attention mechanisms, methods like Probabilistic Attention Keys [Nguyen et al., 2022] and Selective Attention [Leviathan et al., 2024] improve semantic relationship capture and refine attention by suppressing irrelevant features. Additionally, approaches like Differential Transformer address attention noise in long contexts [Ye et al., 2024]. Different from previous work, we improve language modeling by addressing the challenge of periodicity modeling in Transformers, which can seamlessly incorporate the aforementioned works for revising the attention mechanism, as demonstrated in the derivation provided in Appendix L.

Fourier-based Networks Previous research on Fourier-based Networks was aimed at solving some domain-specific applications [Zuo and Cai, 2005, Tan, 2006, Chen et al., 2022, Li et al., 2021]. Some studies specifically explored the use of sinusoidal activations (e.g., cosine [Silvescu, 1999] [Ngom and Marin, 2021] or sine [Parascandolo et al., 2016, Sitzmann et al., 2020]) to approximate periodic patterns [Liu, 2013]. However, these approaches lacked generalizability beyond narrow domains due to rigid frequency parameterization and limited scalability [Uteuliyeva et al., 2020, Liu et al., 2020]. Recent work [Dong et al., 2024a] addresses these problems using FAN to introduce Fourier Principle into neural networks, but its adaptation to LLMs remains an open challenge. FNet [Lee-Thorp et al., 2022] replaces self-attention with Fourier Transform to achieve linear complexity, but it sacrifices the performance of LMs. In contrast, we employ effective periodicity modeling to improve LLMs.

6 Conclusion

We propose FANformer, a novel LLM architecture that enhances learning efficiency by adapting Fourier Analysis Network into attention mechanism for effective periodicity modeling. Experiments show that FANformer outperforms Transformer when scaling model parameters and training tokens, achieving better performance with 31% fewer parameters and 20% fewer tokens. Pretrained FANformer-1B surpasses open-source LLMs of comparable size or training scale on various downstream tasks. The discovery of FANformer’s enhanced scalability, learning efficiency, rule-based learning advantages, and representational capacity suggests potential pathways for developing more efficient and high-performance language models.

7 Acknowledgement

This research is supported by the National Key R&D Program under Grant No. 2023YFB4503801, the National Natural Science Foundation of China under Grant No. 62192733, 62192730, 62192731, the Major Program (JD) of Hubei Province (No.2023BAA024).

References

- Tom B. Brown, Benjamin Mann, Nick Ryder, Melanie Subbiah, Jared Kaplan, Prafulla Dhariwal, Arvind Neelakantan, Pranav Shyam, Girish Sastry, Amanda Askell, Sandhini Agarwal, Ariel Herbert-Voss, Gretchen Krueger, Tom Henighan, Rewon Child, Aditya Ramesh, Daniel M. Ziegler, Jeffrey Wu, Clemens Winter, Christopher Hesse, Mark Chen, Eric Sigler, Mateusz Litwin, Scott Gray, Benjamin Chess, Jack Clark, Christopher Berner, Sam McCandlish, Alec Radford, Ilya Sutskever, and Dario Amodei. Language models are few-shot learners. In *NeurIPS*, 2020.
- Wayne Xin Zhao, Kun Zhou, Junyi Li, Tianyi Tang, Xiaolei Wang, Yupeng Hou, Yingqian Min, Beichen Zhang, Junjie Zhang, Zican Dong, Yifan Du, Chen Yang, Yushuo Chen, Zhipeng Chen, Jinhao Jiang, Ruiyang Ren, Yifan Li, Xinyu Tang, Zikang Liu, Peiyu Liu, Jian-Yun Nie, and Ji-Rong Wen. A survey of large language models. *CoRR*, abs/2303.18223, 2023. doi: 10.48550/ARXIV.2303.18223. URL <https://doi.org/10.48550/arXiv.2303.18223>.
- Shervin Minaee, Tomas Mikolov, Narjes Nikzad, Meysam Chenaghlu, Richard Socher, Xavier Amatriain, and Jianfeng Gao. Large language models: A survey. *CoRR*, abs/2402.06196, 2024. doi: 10.48550/ARXIV.2402.06196. URL <https://doi.org/10.48550/arXiv.2402.06196>.
- OpenAI. GPT-4 technical report. *CoRR*, abs/2303.08774, 2023.
- DeepSeek-AI, Aixin Liu, Bei Feng, Bing Xue, Bingxuan Wang, Bochao Wu, Chengda Lu, Chenggang Zhao, Chengqi Deng, Chenyu Zhang, Chong Ruan, Damai Dai, Daya Guo, Dejian Yang, Deli Chen, Dongjie Ji, Erhang Li, Fangyun Lin, Fucong Dai, Fuli Luo, Guangbo Hao, Guanting Chen, Guowei Li, H. Zhang, Han Bao, Hanwei Xu, Haocheng Wang, Haowei Zhang, Honghui Ding, Huajian Xin, Huazuo Gao, Hui Li, Hui Qu, J. L. Cai, Jian Liang, Jianzhong Guo, Jiaqi Ni, Jiashi Li, Jiawei Wang, Jin Chen, Jingchang Chen, Jingyang Yuan, Junjie Qiu, Junlong Li, Junxiao Song, Kai Dong, Kai Hu, Kaige Gao, Kang Guan, Kexin Huang, Kuai Yu, Lean Wang, Lecong Zhang, Lei Xu, Leyi Xia, Liang Zhao, Litong Wang, Liyue Zhang, Meng Li, Miaojuan Wang, Mingchuan Zhang, Minghua Zhang, Minghui Tang, Mingming Li, Ning Tian, Panpan Huang, Peiyi Wang, Peng Zhang, Qiancheng Wang, Qihao Zhu, Qinyu Chen, Qiushi Du, R. J. Chen, R. L. Jin, Ruiqi Ge, Ruisong Zhang, Ruizhe Pan, Runji Wang, Runxin Xu, Ruoyu Zhang, Ruyi Chen, S. S. Li, Shanghao Lu, Shangyan Zhou, Shanhuang Chen, Shaoqing Wu, Shengfeng Ye, Shengfeng Ye, Shirong Ma, Shiyu Wang, Shuang Zhou, Shuiping Yu, Shunfeng Zhou, Shuting Pan, T. Wang, Tao Yun, Tian Pei, Tianyu Sun, W. L. Xiao, and Wangding Zeng. Deepseek-v3 technical report. *CoRR*, abs/2412.19437, 2024a. doi: 10.48550/ARXIV.2412.19437. URL <https://doi.org/10.48550/arXiv.2412.19437>.
- Dirk Groeneveld, Iz Beltagy, Evan Pete Walsh, Akshita Bhagia, Rodney Kinney, Oyvind Taffjord, Ananya Harsh Jha, Hamish Ivison, Ian Magnusson, Yizhong Wang, Shane Arora, David Atkinson, Russell Authur, Khyathi Raghavi Chandu, Arman Cohan, Jennifer Dumas, Yanai Elazar, Yuling Gu, Jack Hessel, Tushar Khot, William Merrill, Jacob Morrison, Niklas Muennighoff, Aakanksha Naik, Crystal Nam, Matthew E. Peters, Valentina Pyatkin, Abhilasha Ravichander, Dustin Schwenk, Saurabh Shah, Will Smith, Emma Strubell, Nishant Subramani, Mitchell Wortsman, Pradeep Dasigi, Nathan Lambert, Kyle Richardson, Luke Zettlemoyer, Jesse Dodge, Kyle Lo, Luca Soldaini, Noah A. Smith, and Hannaneh Hajishirzi. Olmo: Accelerating the science of language models. In *ACL (1)*, pages 15789–15809. Association for Computational Linguistics, 2024.
- Jared Kaplan, Sam McCandlish, Tom Henighan, Tom B. Brown, Benjamin Chess, Rewon Child, Scott Gray, Alec Radford, Jeffrey Wu, and Dario Amodei. Scaling laws for neural language models. *CoRR*, abs/2001.08361, 2020.
- Jordan Hoffmann, Sebastian Borgeaud, Arthur Mensch, Elena Buchatskaya, Trevor Cai, Eliza Rutherford, Diego de Las Casas, Lisa Anne Hendricks, Johannes Welbl, Aidan Clark, Tom Hennigan, Eric Noland, Katie Millican, George van den Driessche, Bogdan Damoc, Aurelia

- Guy, Simon Osindero, Karen Simonyan, Erich Elsen, Jack W. Rae, Oriol Vinyals, and Laurent Sifre. Training compute-optimal large language models. *CoRR*, abs/2203.15556, 2022. doi: 10.48550/ARXIV.2203.15556. URL <https://doi.org/10.48550/arXiv.2203.15556>.
- Aakanksha Chowdhery, Sharan Narang, Jacob Devlin, Maarten Bosma, Gaurav Mishra, Adam Roberts, Paul Barham, Hyung Won Chung, Charles Sutton, Sebastian Gehrmann, Parker Schuh, Kensen Shi, Sasha Tsvyashchenko, Joshua Maynez, Abhishek Rao, Parker Barnes, Yi Tay, Noam Shazeer, Vinodkumar Prabhakaran, Emily Reif, Nan Du, Ben Hutchinson, Reiner Pope, James Bradbury, Jacob Austin, Michael Isard, Guy Gur-Ari, Pengcheng Yin, Toju Duke, Anselm Levskaya, Sanjay Ghemawat, Sunipa Dev, Henryk Michalewski, Xavier Garcia, Vedant Misra, Kevin Robinson, Liam Fedus, Denny Zhou, Daphne Ippolito, David Luan, Hyeontaek Lim, Barret Zoph, Alexander Spiridonov, Ryan Sepassi, David Dohan, Shivani Agrawal, Mark Omernick, Andrew M. Dai, Thanumalayan Sankaranarayanan Pillai, Marie Pellat, Aitor Lewkowycz, Erica Moreira, Rewon Child, Oleksandr Polozov, Katherine Lee, Zongwei Zhou, Xuezhi Wang, Brennan Saeta, Mark Diaz, Orhan Firat, Michele Catasta, Jason Wei, Kathy Meier-Hellstern, Douglas Eck, Jeff Dean, Slav Petrov, and Noah Fiedel. Palm: Scaling language modeling with pathways. *J. Mach. Learn. Res.*, 24:240:1–240:113, 2023. URL <https://jmlr.org/papers/v24/22-1144.html>.
- Gyorgy Buzsaki. *Rhythms of the Brain*. Oxford university press, 2006.
- Brenden M Lake, Tomer D Ullman, Joshua B Tenenbaum, and Samuel J Gershman. Building machines that learn and think like people. *Behavioral and brain sciences*, 40:e253, 2017.
- Arnaud Zalta, Spase Petkoski, and Benjamin Morillon. Natural rhythms of periodic temporal attention. *Nature communications*, 11(1):1051, 2020.
- Mohammadreza Edalati, Fabrice Wallois, Javad Safaie, Ghida Ghostine, Guy Kongolo, Laurel J Trainor, and Sahar Moghimi. Rhythm in the premature neonate brain: Very early processing of auditory beat and meter. *Journal of Neuroscience*, 43(15):2794–2802, 2023.
- Lexia Zhan, Dingrong Guo, Gang Chen, and Jiongjiong Yang. Effects of repetition learning on associative recognition over time: Role of the hippocampus and prefrontal cortex. *Frontiers in human neuroscience*, 12:277, 2018.
- Yihong Dong, Ge Li, Yongding Tao, Xue Jiang, Kechi Zhang, Jia Li, Jing Su, Jun Zhang, and Jingjing Xu. Fan: Fourier analysis networks. *CoRR*, abs/2410.02675, 2024a.
- Ziyin Liu, Tilman Hartwig, and Masahito Ueda. Neural networks fail to learn periodic functions and how to fix it. In *NeurIPS*, 2020.
- Yihong Dong, Xue Jiang, Yongding Tao, Huanyu Liu, Kechi Zhang, Lili Mou, Rongyu Cao, Yingwei Ma, Jue Chen, Binhua Li, Zhi Jin, Fei Huang, Yongbin Li, and Ge Li. RL-PLUS: countering capability boundary collapse of llms in reinforcement learning with hybrid-policy optimization. *CoRR*, abs/2508.00222, 2025a.
- Yihong Dong, Zhaoyu Ma, Xue Jiang, Zhiyuan Fan, Jiaru Qian, Yongmin Li, Jianha Xiao, Zhi Jin, Rongyu Cao, Binhua Li, Fei Huang, Yongbin Li, and Ge Li. Saber: an efficient sampling with adaptive acceleration and backtracking enhanced remasking for diffusion language model. *CoRR*, abs/2510.18165, 2025b.
- Yi Hu, Xiaojuan Tang, Haotong Yang, and Muhan Zhang. Case-based or rule-based: How do transformers do the math? In *ICML*. OpenReview.net, 2024.
- Siyuan Wang, Zhongyu Wei, Yejin Choi, and Xiang Ren. Can LLMs reason with rules? logic scaffolding for stress-testing and improving LLMs. In Lun-Wei Ku, Andre Martins, and Vivek Srikumar, editors, *Proceedings of the 62nd Annual Meeting of the Association for Computational Linguistics (Volume 1: Long Papers)*, pages 7523–7543, Bangkok, Thailand, August 2024. Association for Computational Linguistics. doi: 10.18653/v1/2024.acl-long.406. URL <https://aclanthology.org/2024.acl-long.406/>.
- Fabian Latorre, Paul Rolland, and Volkan Cevher. Lipschitz constant estimation of neural networks via sparse polynomial optimization. In *ICLR*. OpenReview.net, 2020.

- David S. Dummit and Richard M. Foote. *Abstract Algebra*. John Wiley & Sons, Hoboken, NJ, 3rd edition, 2004. See Sec. 1.7: a group action is *free* iff only the identity fixes any point. Equivalently, if a non-identity $p \in G$ satisfies $p \cdot x = x$, then x is a **periodic** point under the G -action (invariant under $\langle p \rangle$).
- Tri Dao, Daniel Y. Fu, Stefano Ermon, Atri Rudra, and Christopher Ré. Flashattention: Fast and memory-efficient exact attention with io-awareness. In *NeurIPS*, 2022.
- Hugo Touvron, Louis Martin, Kevin Stone, Peter Albert, Amjad Almahairi, Yasmine Babaei, Nikolay Bashlykov, Soumya Batra, Prajwal Bhargava, Shruti Bhosale, Dan Bikel, Lukas Blecher, Cristian Canton-Ferrer, Moya Chen, Guillem Cucurull, David Esiobu, Jude Fernandes, Jeremy Fu, Wenyin Fu, Brian Fuller, Cynthia Gao, Vedanuj Goswami, Naman Goyal, Anthony Hartshorn, Saghar Hosseini, Rui Hou, Hakan Inan, Marcin Kardas, Viktor Kerkez, Madian Khabsa, Isabel Kloumann, Artem Korenev, Punit Singh Koura, Marie-Anne Lachaux, Thibaut Lavril, Jenya Lee, Diana Liskovich, Yinghai Lu, Yuning Mao, Xavier Martinet, Todor Mihaylov, Pushkar Mishra, Igor Molybog, Yixin Nie, Andrew Poulton, Jeremy Reizenstein, Rashi Rungta, Kalyan Saladi, Alan Schelten, Ruan Silva, Eric Michael Smith, Ranjan Subramanian, Xiaoqing Ellen Tan, Binh Tang, Ross Taylor, Adina Williams, Jian Xiang Kuan, Puxin Xu, Zheng Yan, Iliyan Zarov, Yuchen Zhang, Angela Fan, Melanie Kambadur, Sharan Narang, Aurélien Rodriguez, Robert Stojnic, Sergey Edunov, and Thomas Scialom. Llama 2: Open foundation and fine-tuned chat models. *CoRR*, abs/2307.09288, 2023a.
- Prajit Ramachandran, Barret Zoph, and Quoc V. Le. Searching for activation functions. In *ICLR (Workshop)*. OpenReview.net, 2018.
- Noam Shazeer. GLU variants improve transformer. *CoRR*, abs/2002.05202, 2020.
- Biao Zhang and Rico Sennrich. Root mean square layer normalization. In *NeurIPS*, pages 12360–12371, 2019.
- Luca Soldaini, Rodney Kinney, Akshita Bhagia, Dustin Schwenk, David Atkinson, Russell Authur, Ben Bogin, Khyathi Raghavi Chandu, Jennifer Dumas, Yanai Elazar, Valentin Hofmann, Ananya Harsh Jha, Sachin Kumar, Li Lucy, Xinxu Lyu, Nathan Lambert, Ian Magnusson, Jacob Morrison, Niklas Muennighoff, Aakanksha Naik, Crystal Nam, Matthew E. Peters, Abhilasha Ravichander, Kyle Richardson, Zejiang Shen, Emma Strubell, Nishant Subramani, Oyvind Tafjord, Pete Walsh, Luke Zettlemoyer, Noah A. Smith, Hannaneh Hajishirzi, Iz Beltagy, Dirk Groeneveld, Jesse Dodge, and Kyle Lo. Dolma: an open corpus of three trillion tokens for language model pretraining research. In *ACL (1)*, pages 15725–15788. Association for Computational Linguistics, 2024.
- AllenAI. Dolma, 2023. URL <https://huggingface.co/datasets/allenai/dolma>.
- Hugo Touvron, Thibaut Lavril, Gautier Izacard, Xavier Martinet, Marie-Anne Lachaux, Timothée Lacroix, Baptiste Rozière, Naman Goyal, Eric Hambro, Faisal Azhar, Aurélien Rodriguez, Armand Joulin, Edouard Grave, and Guillaume Lample. Llama: Open and efficient foundation language models. *CoRR*, abs/2302.13971, 2023b.
- Peter Clark, Isaac Cowhey, Oren Etzioni, Tushar Khot, Ashish Sabharwal, Carissa Schoenick, and Oyvind Tafjord. Think you have solved question answering? try arc, the AI2 reasoning challenge. *CoRR*, abs/1803.05457, 2018.
- Christopher Clark, Kenton Lee, Ming-Wei Chang, Tom Kwiatkowski, Michael Collins, and Kristina Toutanova. Boolq: Exploring the surprising difficulty of natural yes/no questions. In *NAACL-HLT (1)*, pages 2924–2936. Association for Computational Linguistics, 2019.
- Rowan Zellers, Ari Holtzman, Yonatan Bisk, Ali Farhadi, and Yejin Choi. Hellaswag: Can a machine really finish your sentence? In *ACL (1)*, pages 4791–4800. Association for Computational Linguistics, 2019.
- Todor Mihaylov, Peter Clark, Tushar Khot, and Ashish Sabharwal. Can a suit of armor conduct electricity? A new dataset for open book question answering. In *EMNLP*, pages 2381–2391. Association for Computational Linguistics, 2018.

- Yonatan Bisk, Rowan Zellers, Ronan Le Bras, Jianfeng Gao, and Yejin Choi. PIQA: reasoning about physical commonsense in natural language. In *AAAI*, pages 7432–7439. AAAI Press, 2020.
- Johannes Welbl, Nelson F. Liu, and Matt Gardner. Crowdsourcing multiple choice science questions. In *NUT@EMNLP*, pages 94–106. Association for Computational Linguistics, 2017.
- Keisuke Sakaguchi, Ronan Le Bras, Chandra Bhagavatula, and Yejin Choi. Winogrande: An adversarial winograd schema challenge at scale. In *AAAI*, pages 8732–8740. AAAI Press, 2020.
- Qwen Team. Qwen2.5: A party of foundation models, September 2024. URL <https://qwenlm.github.io/blog/qwen2.5/>.
- DeepSeek-AI, Daya Guo, Dejian Yang, Haowei Zhang, Junxiao Song, Ruoyu Zhang, Runxin Xu, Qihao Zhu, Shirong Ma, Peiyi Wang, Xiao Bi, et al. Deepseek-r1: Incentivizing reasoning capability in llms via reinforcement learning. *arXiv preprint arXiv:2501.12948*, 2025.
- Abhimanyu Dubey, Abhinav Jauhri, Abhinav Pandey, Abhishek Kadian, Ahmad Al-Dahle, Aiesha Letman, Akhil Mathur, Alan Schelten, Amy Yang, Angela Fan, Anirudh Goyal, Anthony Hartshorn, Aobo Yang, Archi Mitra, Archie Sravankumar, Artem Korenev, Arthur Hinsvark, Arun Rao, Aston Zhang, Aurélien Rodriguez, Austen Gregerson, Ava Spataru, Baptiste Rozière, Bethany Biron, Binh Tang, Bobbie Chern, Charlotte Caucheteux, Chaya Nayak, Chloe Bi, Chris Marra, Chris McConnell, Christian Keller, Christophe Touret, Chunyang Wu, Corinne Wong, Cristian Canton Ferrer, Cyrus Nikolaidis, Damien Allonsius, Daniel Song, Danielle Pintz, Danny Livshits, David Esiobu, Dhruv Choudhary, Dhruv Mahajan, Diego Garcia-Olano, Diego Perino, Dieuwke Hupkes, Egor Lakomkin, Ehab AlBadawy, Elina Lobanova, Emily Dinan, Eric Michael Smith, Filip Radenovic, Frank Zhang, Gabriel Synnaeve, Gabrielle Lee, Georgia Lewis Anderson, Graeme Nail, Grégoire Mialon, Guan Pang, Guillem Cucurell, Hailey Nguyen, Hannah Korevaar, Hu Xu, Hugo Touvron, Iliyan Zarov, Imanol Arrieta Ibarra, Isabel M. Kloumann, Ishan Misra, Ivan Evtimov, Jade Copet, Jaewon Lee, Jan Geffert, Jana Vranes, Jason Park, Jay Mahadeokar, Jeet Shah, Jelmer van der Linde, Jennifer Billock, Jenny Hong, Jenya Lee, Jeremy Fu, Jianfeng Chi, Jianyu Huang, Jiawen Liu, Jie Wang, Jiecao Yu, Joanna Bitton, Joe Spisak, Jongsoo Park, Joseph Rocca, Joshua Johnstun, Joshua Saxe, Junteng Jia, Kalyan Vasuden Alwala, Kartikeya Upasani, Kate Plawiak, Ke Li, Kenneth Heafield, Kevin Stone, and et al. The llama 3 herd of models. *CoRR*, abs/2407.21783, 2024.
- Peiyuan Zhang, Guangtao Zeng, Tianduo Wang, and Wei Lu. Tinyllama: An open-source small language model. *CoRR*, abs/2401.02385, 2024.
- Xinyang Geng and Hao Liu. Openllama: An open reproduction of llama, May 2023. URL https://github.com/openlm-research/open_llama.
- Jonathan Tow. Stablelm alpha v2 models, 2023. URL <https://huggingface.co/stabilityai/stablelm-base-alpha-3b-v2>.
- Tianzhu Ye, Li Dong, Yuqing Xia, Yutao Sun, Yi Zhu, Gao Huang, and Furu Wei. Differential transformer. *CoRR*, abs/2410.05258, 2024.
- Xin Dong, Yonggan Fu, Shizhe Diao, Wonmin Byeon, Zijia Chen, Ameya Sunil Mahabaleshwar, Shih-Yang Liu, Matthijs Van Keirsbilck, Min-Hung Chen, Yoshi Suhara, Yingyan Lin, Jan Kautz, and Pavlo Molchanov. Hymba: A hybrid-head architecture for small language models. *CoRR*, abs/2411.13676, 2024b.
- Yihong Dong, Xue Jiang, Huanyu Liu, Zhi Jin, Bin Gu, Mengfei Yang, and Ge Li. Generalization or memorization: Data contamination and trustworthy evaluation for large language models. In *ACL (Findings)*, pages 12039–12050. Association for Computational Linguistics, 2024c.
- Graham Priest, Jeffrey C Beall, and Bradley Armour-Garb. *The law of non-contradiction: New philosophical essays*. Clarendon Press, 2006.
- Peter L. Bartlett, Dylan J. Foster, and Matus Telgarsky. Spectrally-normalized margin bounds for neural networks. In *NIPS*, pages 6240–6249, 2017.

- Alec Radford. Improving language understanding by generative pre-training. 2018.
- Xiao Bi, Deli Chen, Guanting Chen, Shanhuang Chen, Damai Dai, Chengqi Deng, Honghui Ding, Kai Dong, Qiushi Du, Zhe Fu, Huazuo Gao, Kaige Gao, Wenjun Gao, Ruiqi Ge, Kang Guan, Daya Guo, Jianzhong Guo, Guangbo Hao, Zhewen Hao, Ying He, Wenjie Hu, Panpan Huang, Erhang Li, Guowei Li, Jiashi Li, Yao Li, Y. K. Li, Wenfeng Liang, Fangyun Lin, Alex X. Liu, Bo Liu, Wen Liu, Xiaodong Liu, Xin Liu, Yiyuan Liu, Haoyu Lu, Shanghao Lu, Fuli Luo, Shirong Ma, Xiaotao Nie, Tian Pei, Yishi Piao, Junjie Qiu, Hui Qu, Tongzheng Ren, Zehui Ren, Chong Ruan, Zhangli Sha, Zhihong Shao, Junxiao Song, Xuecheng Su, Jingxiang Sun, Yaofeng Sun, Minghui Tang, Bingxuan Wang, Peiyi Wang, Shiyu Wang, Yaohui Wang, Yongji Wang, Tong Wu, Y. Wu, Xin Xie, Zhenda Xie, Ziwei Xie, Yiliang Xiong, Hanwei Xu, R. X. Xu, Yanhong Xu, Dejian Yang, Yuxiang You, Shuiping Yu, Xingkai Yu, B. Zhang, Haowei Zhang, Lecong Zhang, Liyue Zhang, Mingchuan Zhang, Minghua Zhang, Wentao Zhang, Yichao Zhang, Chenggang Zhao, Yao Zhao, Shangyan Zhou, Shunfeng Zhou, Qihao Zhu, and Yuheng Zou. Deepseek LLM: scaling open-source language models with longtermism. *CoRR*, abs/2401.02954, 2024.
- Rewon Child, Scott Gray, Alec Radford, and Ilya Sutskever. Generating long sequences with sparse transformers. *CoRR*, abs/1904.10509, 2019.
- Iz Beltagy, Matthew E. Peters, and Arman Cohan. Longformer: The long-document transformer. *CoRR*, abs/2004.05150, 2020.
- Noam Shazeer. Fast transformer decoding: One write-head is all you need. *CoRR*, abs/1911.02150, 2019.
- Joshua Ainslie, James Lee-Thorp, Michiel de Jong, Yury Zemlyanskiy, Federico Lebrón, and Sumit Sanghai. GQA: training generalized multi-query transformer models from multi-head checkpoints. In *EMNLP*, pages 4895–4901. Association for Computational Linguistics, 2023.
- DeepSeek-AI, Aixin Liu, Bei Feng, Bin Wang, Bingxuan Wang, Bo Liu, Chenggang Zhao, Chengqi Deng, Chong Ruan, Damai Dai, Daya Guo, Dejian Yang, Deli Chen, Dongjie Ji, Erhang Li, Fangyun Lin, Fuli Luo, Guangbo Hao, Guanting Chen, Guowei Li, Hao Zhang, Hanwei Xu, Hao Yang, Haowei Zhang, Honghui Ding, Huajian Xin, Huazuo Gao, Hui Li, Hui Qu, J. L. Cai, Jian Liang, Jianzhong Guo, Jiaqi Ni, Jiashi Li, Jin Chen, Jingyang Yuan, Junjie Qiu, Junxiao Song, Kai Dong, Kaige Gao, Kang Guan, Lean Wang, Lecong Zhang, Lei Xu, Leyi Xia, Liang Zhao, Liyue Zhang, Meng Li, Miaojun Wang, Mingchuan Zhang, Minghua Zhang, Minghui Tang, Mingming Li, Ning Tian, Panpan Huang, Peiyi Wang, Peng Zhang, Qihao Zhu, Qinyu Chen, Qiushi Du, R. J. Chen, R. L. Jin, Ruiqi Ge, Ruizhe Pan, Runxin Xu, Ruyi Chen, S. S. Li, Shanghao Lu, Shangyan Zhou, Shanhuang Chen, Shaoqing Wu, Shengfeng Ye, Shirong Ma, Shiyu Wang, Shuang Zhou, Shuiping Yu, Shunfeng Zhou, Size Zheng, Tao Wang, Tian Pei, Tian Yuan, Tianyu Sun, W. L. Xiao, Wangding Zeng, Wei An, Wen Liu, Wenfeng Liang, Wenjun Gao, Wentao Zhang, X. Q. Li, Xiangyue Jin, Xianzu Wang, Xiao Bi, Xiaodong Liu, Xiaohan Wang, Xiaojin Shen, Xiaokang Chen, Xiaosha Chen, Xiaotao Nie, and Xiaowen Sun. Deepseek-v2: A strong, economical, and efficient mixture-of-experts language model. *CoRR*, abs/2405.04434, 2024b.
- Tam Minh Nguyen, Tan Minh Nguyen, Dung D. D. Le, Duy Khuong Nguyen, Viet-Anh Tran, Richard G. Baraniuk, Nhat Ho, and Stanley J. Osher. Improving transformers with probabilistic attention keys. In *ICML*, volume 162 of *Proceedings of Machine Learning Research*, pages 16595–16621. PMLR, 2022.
- Yaniv Leviathan, Matan Kalman, and Yossi Matias. Selective attention improves transformer. *CoRR*, abs/2410.02703, 2024.
- Wei Zuo and Lilong Cai. Tracking control of nonlinear systems using fourier neural network. In *Proceedings, 2005 IEEE/ASME International Conference on Advanced Intelligent Mechatronics.*, pages 670–675. IEEE, 2005.
- HS Tan. Fourier neural networks and generalized single hidden layer networks in aircraft engine fault diagnostics. 2006.
- Hanlong Chen, Luzhe Huang, Tairan Liu, and Aydogan Ozcan. Fourier imager network (FIN): A deep neural network for hologram reconstruction with superior external generalization. *Light: Science & Applications*, 2022.

- Zongyi Li, Nikola Borislavov Kovachki, Kamyar Azizzadenesheli, Burigede Liu, Kaushik Bhattacharya, Andrew M. Stuart, and Anima Anandkumar. Fourier neural operator for parametric partial differential equations. In *ICLR*. OpenReview.net, 2021.
- Adrian Silvescu. Fourier neural networks. In *IJCNN'99. International Joint Conference on Neural Networks. Proceedings (Cat. No. 99CH36339)*, volume 1, pages 488–491. IEEE, 1999.
- Marieme Ngom and Oana Marin. Fourier neural networks as function approximators and differential equation solvers. *Statistical Analysis and Data Mining: The ASA Data Science Journal*, 14(6): 647–661, 2021.
- Giambattista Parascandolo, Heikki Huttunen, and Tuomas Virtanen. Taming the waves: sine as activation function in deep neural networks. 2016.
- Vincent Sitzmann, Julien Martel, Alexander Bergman, David Lindell, and Gordon Wetzstein. Implicit neural representations with periodic activation functions. *Advances in neural information processing systems*, 33:7462–7473, 2020.
- Shuang Liu. Fourier neural network for machine learning. In *2013 international conference on machine learning and cybernetics*, volume 1, pages 285–290. IEEE, 2013.
- Malika Uteuliyeva, Abylay Zhumekenov, Rustem Takhanov, Zhenisbek Assylbekov, Alejandro J. Castro, and Olzhas Kabdolov. Fourier neural networks: A comparative study. *Intell. Data Anal.*, 24(5):1107–1120, 2020.
- James Lee-Thorp, Joshua Ainslie, Ilya Eckstein, and Santiago Ontañón. Fnet: Mixing tokens with fourier transforms. In *NAACL-HLT*, pages 4296–4313. Association for Computational Linguistics, 2022.
- Albert Gu and Tri Dao. Mamba: Linear-time sequence modeling with selective state spaces. *CoRR*, abs/2312.00752, 2023.
- Samyam Rajbhandari, Jeff Rasley, Olatunji Ruwase, and Yuxiong He. Zero: memory optimizations toward training trillion parameter models. In *SC*, page 20. IEEE/ACM, 2020.
- Shen Li. Getting started with distributed data parallel, 2018. URL https://pytorch.org/tutorials/intermediate/ddp_tutorial.html.
- Ilya Loshchilov and Frank Hutter. Decoupled weight decay regularization. In *ICLR (Poster)*. OpenReview.net, 2019.
- Defa Zhu, Hongzhi Huang, Zihao Huang, Yutao Zeng, Yunyao Mao, Banggu Wu, Qiyang Min, and Xun Zhou. Hyper-connections. *CoRR*, abs/2409.19606, 2024.
- Melissa Roemmele, Cosmin Adrian Bejan, and Andrew S. Gordon. Choice of plausible alternatives: An evaluation of commonsense causal reasoning. In *AAAI Spring Symposium: Logical Formalizations of Commonsense Reasoning*. AAAI, 2011.
- Marie-Catherine De Marneffe, Mandy Simons, and Judith Tonhauser. The commitmentbank: Investigating projection in naturally occurring discourse. In *proceedings of Sinn und Bedeutung*, volume 23, pages 107–124, 2019.
- William B. Dolan and Chris Brockett. Automatically constructing a corpus of sentential paraphrases. In *IWP@IJCNLP*. Asian Federation of Natural Language Processing, 2005.
- Ido Dagan, Oren Glickman, and Bernardo Magnini. The PASCAL recognising textual entailment challenge. In *MLCW*, volume 3944 of *Lecture Notes in Computer Science*, pages 177–190. Springer, 2005.
- Richard Socher, Alex Perelygin, Jean Wu, Jason Chuang, Christopher D. Manning, Andrew Y. Ng, and Christopher Potts. Recursive deep models for semantic compositionality over a sentiment treebank. In *EMNLP*, pages 1631–1642. ACL, 2013.
- Jason Wei, Xuezhi Wang, Dale Schuurmans, Maarten Bosma, Fei Xia, Ed Chi, Quoc V Le, Denny Zhou, et al. Chain-of-thought prompting elicits reasoning in large language models. *Advances in Neural Information Processing Systems*, 35:24824–24837, 2022.

A Training Loss Curves of OLMo and FANformer

We present the training loss curves for OLMo and FANformer trained on 1 trillion tokens (i.e., 250K steps) in Figure 7.

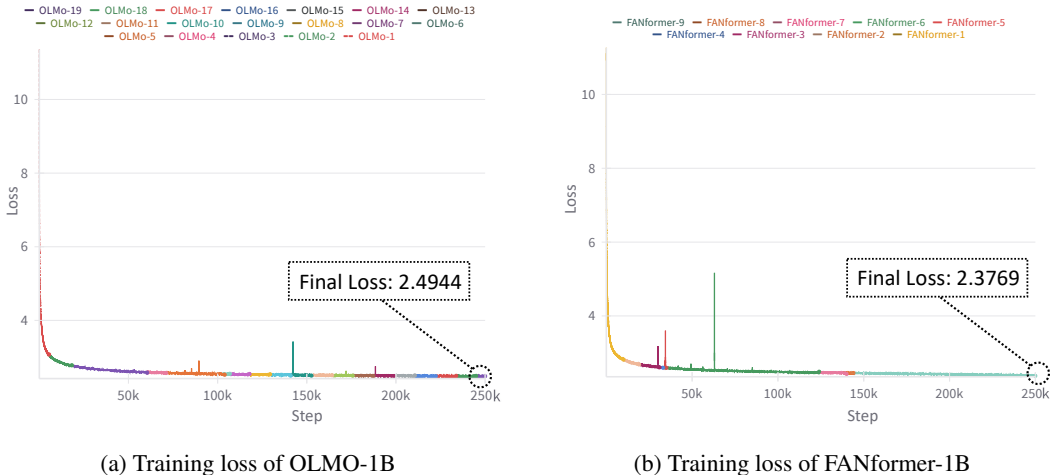


Figure 7: The training process of OLMo and FANformer. The data in Figure (a) is sourced from the publicly available results of OLMo (<https://wandb.ai/ai2-11m/OLMo-1B?nw=nwuserdirkgr>).

B Preliminary Knowledge

Fourier Analysis Network (FAN) [Dong et al., 2024a] enhances neural networks by introducing Fourier principles for effective periodicity modeling. The core component of FAN is its layer design, which combines periodic basis functions with standard linear transformations. Given an input \mathbf{X} , the FAN layer is defined as:

$$\text{FANLayer}(\mathbf{X}) = [\cos(W_p \mathbf{X}) \parallel \sin(W_p \mathbf{X}) \parallel \sigma(W_{\bar{p}} \mathbf{X} + B_{\bar{p}})] \quad (10)$$

where W_p and $W_{\bar{p}}$ are learnable projection matrices, $B_{\bar{p}}$ is a bias term, σ denotes an activation function, and \parallel represents concatenation. Compared to MLP layer, FAN layer explicitly encodes periodic patterns through Fourier series while maintaining general-purpose modeling capabilities.

C Experiments on Code Generation and Math tasks

We conduct experiments on code generation tasks (i.e., HumanEval and MBPP) and human-written math tasks (i.e., GSM8K) compared to our baseline, OLMo [Groeneveld et al., 2024]. The results show that our FANformer achieves clear and consistent improvements compared with OLMo on all three benchmarks.

Table 4: Comparison of LLMs on coding and math benchmarks.

LLMs	Training Tokens	HumanEval	MBPP	GSM8K
OLMo-1B	3T checkpoint	5.2	3.1	8.9
FANformer-1B	1T from scratch	6.3	5.4	15.7

D Effect of hyperparameter p

We systematically investigate the impact of hyperparameter p , which controls the proportion of periodicity modeling in FANformer, on model performance across its value range. The experimental results from the 1B-scale FANformer (as shown in Figure 8) demonstrate that our model exhibits

strong robustness in terms of training loss and downstream task accuracy, with relatively small performance fluctuations. Furthermore, regardless of the variation in p -values, FANformer consistently outperforms the standard Transformer (horizontal baseline). Analysis of experimental results from models of different scales (300M, 1B, 3B) (as shown in Figure 9) reveals a clear trend: larger models tend to exhibit higher optimal p values. This observation suggests that more powerful FANformers are better equipped to extract more intricate latent periodicity features.

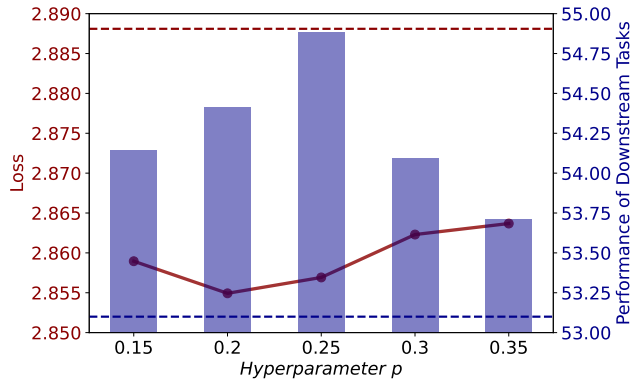


Figure 8: Effect of hyperparameter p in FANformer on its training loss and downstream task performance, where the red dashed line represents the training loss of Transformer, while the blue dashed line denotes the performance on downstream tasks of Transformer.

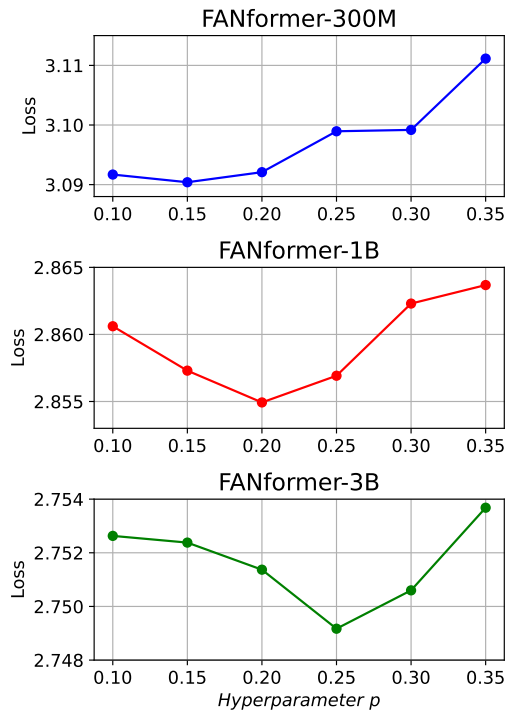


Figure 9: The impact of hyperparameter p on FANformer models of varying sizes.

Table 5: Evaluation results of OLMo-1B-SFT and FANformer-1B-SFT on MMLU, AlpacaEval, ToxiGen, and TruthfulQA (Info+True). Higher values are better for MMLU, AlpacaEval, and TruthfulQA, while lower values are better for ToxiGen.

Model	MMLU	AlpacaEval	ToxiGen	TruthfulQA (Info+True)
	0-shot \uparrow	% win \uparrow	% Toxic \downarrow	Accuracy \uparrow
OLMo-1B-SFT	24.3	1.90	2.8	55.8
FANformer-1B-SFT	26.7	2.51	10.4	83.0

E Instruction Following with SFT

E.1 Models

FANformer-1B-SFT: Our pretrained model on 1 trillion tokens, fine-tuned using supervised fine-tuning (SFT) on the `tulu-3-sft-olmo-2-mixture` dataset.

OLMo-1B-SFT: A 1B parameter version of OLMo, pre-trained on 3 trillion tokens and fine-tuned using supervised fine-tuning (SFT) on the `tulu-3-sft-olmo-2-mixture` dataset. Model available at `allenai/OLMo-1B-hf`.

For both models, we follow the tokenizer’s chat template for prompt formatting when available.

E.2 Evaluation Setup

We evaluate the models on four benchmarks: MMLU, TruthfulQA, AlpacaEval, and ToxiGen. The evaluation is conducted using the `open-instruct` evaluation suite, which has been widely adopted for evaluating instruction-tuned language models. Below, we describe the setup for each benchmark.

MMLU We use the official MMLU evaluation script with 0-shot prompting. The maximum token length is set to 2048, and we do not employ chain-of-thought (CoT) reasoning. The evaluation reports the average accuracy across test examples.

AlpacaEval We use the AlpacaEval V1 benchmark with the default setup from the official repository². The evaluated models generate responses for 805 prompts, and GPT-4 is employed to compare the responses with those from the reference model (`gpt-4-1106-preview`). Given the updates in the AlpacaEval repository, the default models have changed over time. Currently, the default setup uses the `weighted_alpaca_eval_gpt4_turbo` annotator as the annotator and `gpt-4-1106-preview` as the reference model. Therefore, our evaluation aligns with the current default configuration in the official AlpacaEval repository.

ToxiGen For ToxiGen, we focus on the prompts specifically designed to elicit toxic language (‘hateful’ prompts). To reduce evaluation costs, we use a subset of 500 prompts per group for testing. The toxicity classifier used is `toxigen_roberta`. We report the percentage of generations classified as toxic by the classifier.

TruthfulQA For TruthfulQA, we use the generation setting with the default QA prompt format, including 6 in-context examples. The judge model for evaluating truthfulness and informativeness is `allenai/truthfulqa-truth-judge-llama2-7B`, which is adopted in the `open-instruct` evaluation suite and OLMo’s evaluation. We report the percentage of responses deemed both informative and truthful.

F Computational Cost Analysis

We analyze the computational overhead of FANformer compared to standard Transformer under two settings: (1) when the number of parameters is matched, the computational cost remains unchanged; (2) when the FFN dimensions remain fixed, the increase in cost is negligible.

²https://github.com/tatsu-lab/alpaca_eval

To ensure a fair comparison, we maintain the same number of parameters in FANformer as in the original Transformer by varying the FFN’s intermediate dimension d_f during our experiments. Under this configuration, the computational cost remains equivalent between FANformer (same parameter) and Transformer. We further investigate the setting where FFN dimensions remain unchanged (Table 6). Even for FANformer (same dimension), the computational cost increases only slightly compared to the Transformer. Specifically, the ratio of additional computation can be expressed as:

$$\frac{1.5LSD^2}{L \times (24SD^2 + 4S^2D) + 2SDV} = \frac{1.5D}{24D + 4S} \leq \frac{1.5D}{24D} = 0.0625, \quad (11)$$

where L is the number of layers, S is the sequence length, D is the hidden dimension, and V is the vocabulary size. In practice, the actual additional overhead is much lower than 0.0625, as the term scales inversely with sequence length. This means the overhead diminishes rapidly as sequences grow longer. We summarize the detailed comparison of computational costs between Transformer and FANformer in Table 6.

Table 6: Computational cost of Transformer vs. FANformer ($p = 0.25$).

Model	Self-Attention/ATF FLOPs	FFN FLOPs	Output FLOPs	Total FLOPs
Transformer	$L \times (8SD^2 + 4S^2D)$	$L \times 16SD^2$	$2SDV$	$L \times (24SD^2 + 4S^2D) + 2SDV$
FANformer (Same Param)	$L \times (8SD^2 + 4S^2D + 1.5SD^2)$	$L \times (16SD^2 - 1.5SD^2)$	$2SDV$	$L \times (24SD^2 + 4S^2D) + 2SDV$
FANformer (Same Dim)	$L \times (8SD^2 + 4S^2D + 1.5SD^2)$	$L \times 16SD^2$	$2SDV$	$L \times (25.5SD^2 + 4S^2D) + 2SDV$

G Inference Speed and GPU Memory Usage

We conduct experiments on the inference speed and GPU memory usage of FANformer relative to Transformer in deployment settings, and have added the experimental results to our revised manuscript. The results show that it add little latency. The configuration of benchmark test: we run for 20 iterations on a single GPU of A100 80G with a fixed sequence length of 4096 tokens and float16 precision.

Table 7: Inference speed and memory usage comparison (Sequence Length=4096).

Metric	OLMo-1B	FANformer-1B	Difference
Forward Pass Time	141.49 ms	142.88 ms	+1.39 ms (+0.98%)
Allocated Memory	4642.69 MB	4738.86 MB	+96.17 MB (+2.1%)
Peak Memory	6610.70 MB	6706.88 MB	+96.18 MB (+1.5%)

H Different with Mamba

First, our approach is fundamentally different from SSMS. SSMS model periodicity along the sequence dimension, while our FANformer models it along the feature dimension. Second, our motivation is distinct from that of Mamba. Mamba [Gu and Dao, 2023] is primarily developed to overcome the quadratic computational complexity of Transformers and improve inference efficiency, while our approach is designed to improve learning efficiency and performance of Transformers through effective periodicity modeling.

I Detailed Results of Ablation Study for Section 4.4.1

In ablation study, we report the average results across various tasks on V2 Validation Sets, V3 Validation Sets, and Downstream tasks, with the specific tasks detailed in Section M.3. The complete results are detailed in Table 8 and Table 9.

J Extended results of Section 4.4.3

The training and testing performance metrics, including loss and accuracy, for case-based and rule-based reasoning are presented in Figure 11 and Figure 12, respectively.

Table 8: The detailed results of ablation study (Part One). All models keep the same number of parameters and are pretrained on Dolma v1_6-sample dataset (about 10B tokens).

			Transformer	Transformer + ATM	Transformer + ATL	FANformer + Activation	FANformer	
V2 Validation Sets	4chan	Loss	2.68	2.68	2.66	2.70	2.66	
		PPL	14.60	14.53	14.36	14.88	14.34	
	c4_100_domains	Loss	3.11	3.11	3.10	3.12	3.08	
		PPL	22.38	22.52	22.18	22.63	21.87	
	c4_en	Loss	3.27	3.28	3.27	3.29	3.25	
		PPL	26.40	26.54	26.22	26.78	25.85	
	gab	Loss	3.90	3.90	3.89	3.91	3.87	
		PPL	49.58	49.64	49.11	50.05	47.83	
	ice	Loss	3.20	3.21	3.19	3.21	3.17	
		PPL	24.59	24.77	24.25	24.82	23.93	
	m2d2_s2orc	Loss	3.56	3.57	3.56	3.59	3.56	
		PPL	35.34	35.47	34.99	36.24	35.05	
	m2d2_wiki	Loss	3.14	3.14	3.13	3.15	3.11	
		PPL	23.17	23.13	22.90	23.29	22.48	
	manosphere	Loss	3.47	3.48	3.46	3.48	3.45	
		PPL	32.21	32.46	31.85	32.62	31.48	
	mc4_en	Loss	3.02	3.02	3.01	3.03	2.99	
		PPL	20.53	20.52	20.22	20.76	19.91	
	pile	Loss	2.76	2.76	2.74	2.77	2.73	
		PPL	15.84	15.74	15.53	15.99	15.30	
	ptb	Loss	3.68	3.70	3.64	3.71	3.66	
		PPL	39.68	40.51	38.23	40.74	38.75	
	twitterAEE	Loss	4.10	4.10	4.07	4.11	4.07	
		PPL	60.25	60.18	58.79	61.10	58.54	
	wikitext_103	Loss	3.33	3.33	3.30	3.35	3.29	
		PPL	28.03	28.07	27.15	28.48	26.88	
Average	Loss	3.33	3.33	3.31	3.34	3.30		
	PPL	30.20	30.31	29.68	30.64	29.40		
V3 Validation Sets	c4_en	Loss	3.21	3.21	3.20	3.22	3.19	
		PPL	24.80	24.86	24.60	25.04	24.24	
	dolma_books	Loss	3.56	3.56	3.54	3.57	3.52	
		PPL	34.98	35.32	34.43	35.57	33.96	
	dolma_common-crawl	Loss	3.23	3.24	3.23	3.24	3.21	
		PPL	25.32	25.42	25.16	25.47	24.76	
	dolma_pes2o	Loss	2.86	2.85	2.84	2.86	2.83	
		PPL	17.45	17.35	17.09	17.53	16.88	
	dolma_reddit	Loss	3.44	3.44	3.43	3.45	3.42	
		PPL	31.13	31.35	30.94	31.42	30.54	
	dolma_stack	Loss	1.42	1.41	1.40	1.42	1.39	
		PPL	4.13	4.10	4.06	4.13	4.01	
	dolma_wiki	Loss	3.04	3.04	3.03	3.04	3.01	
		PPL	20.89	20.84	20.62	20.97	20.26	
	ice	Loss	3.19	3.20	3.18	3.20	3.17	
		PPL	24.41	24.56	24.09	24.63	23.75	
	m2d2_s2orc	Loss	3.70	3.70	3.69	3.70	3.68	
		PPL	40.35	40.61	40.22	40.56	39.50	
	pile	Loss	2.74	2.73	2.72	2.75	2.70	
		PPL	15.44	15.35	15.16	15.58	14.92	
	wikitext_103	Loss	3.34	3.34	3.31	3.35	3.30	
		PPL	28.21	28.21	27.33	28.57	27.03	
	Average	Loss	3.07	3.07	3.05	3.07	3.04	
		PPL	24.28	24.36	23.97	24.50	23.62	
	Downstream Benchmarks	pqa	ACC	66.43	66.54	65.45	66.10	66.45
			ACC	33.87	33.84	34.02	33.75	34.37
hellaswag		ACC	52.80	51.62	49.96	48.78	51.72	
		ACC	28.00	28.20	28.00	28.20	29.00	
openbook_qa		ACC	70.30	72.10	69.00	67.20	71.80	
		ACC	45.44	46.14	47.19	47.02	45.61	
copa		ACC	62.00	66.00	65.00	66.00	66.00	
		ACC	51.26	52.35	52.71	48.74	57.04	
commitment_bank		ACC	42.86	41.07	46.43	53.57	44.64	
		ACC	81.05	81.22	81.22	81.22	81.47	
mrpc		ACC	50.11	51.49	49.08	49.08	59.11	
		ACC	53.10	53.69	53.46	53.61	55.19	

Table 9: The detailed results of ablation study (Part Two). All models keep the same dimension and are pretrained on Dolma v1_6-sample dataset (about 10B tokens).

			Transformer	Transformer + ATM	Transformer + ATL	FANformer + Activation	FANformer	
V2 Validation Sets	4chan	Loss	2.68	2.68	2.67	2.68	2.66	
		PPL	14.60	14.54	14.43	14.63	14.29	
	c4_100_domains	Loss	3.11	3.11	3.10	3.11	3.08	
		PPL	22.38	22.43	22.11	22.49	21.69	
	c4_en	Loss	3.27	3.28	3.26	3.28	3.24	
		PPL	26.40	26.51	26.12	26.54	25.61	
	gab	Loss	3.90	3.90	3.89	3.91	3.87	
		PPL	49.58	49.41	48.97	50.11	47.79	
	ice	Loss	3.20	3.20	3.19	3.21	3.17	
		PPL	24.59	24.62	24.22	24.90	23.69	
	m2d2_s2orc	Loss	3.56	3.58	3.56	3.58	3.54	
		PPL	35.34	35.73	35.17	35.78	34.58	
	m2d2_wiki	Loss	3.14	3.14	3.13	3.14	3.10	
		PPL	23.17	23.04	22.81	23.10	22.27	
	manosphere	Loss	3.47	3.48	3.46	3.48	3.45	
		PPL	32.21	32.44	31.78	32.43	31.36	
	mc4_en	Loss	3.02	3.02	3.01	3.03	2.99	
		PPL	20.53	20.51	20.22	20.61	19.86	
	pile	Loss	2.76	2.76	2.74	2.77	2.72	
		PPL	15.84	15.78	15.54	15.90	15.24	
	ptb	Loss	3.68	3.67	3.67	3.73	3.63	
		PPL	39.68	39.19	39.15	41.67	37.82	
	twitterAEE	Loss	4.10	4.10	4.08	4.11	4.07	
		PPL	60.25	60.19	59.12	60.97	58.62	
	wikitext_103	Loss	3.33	3.33	3.31	3.34	3.29	
		PPL	28.03	27.96	27.29	28.22	26.98	
Average	Loss	3.33	3.33	3.31	3.34	3.29		
	PPL	30.20	30.18	29.76	30.57	29.22		
V3 Validation Sets	c4_en	Loss	3.21	3.21	3.20	3.21	3.18	
		PPL	24.80	24.78	24.52	24.82	24.00	
	dolma_books	Loss	3.56	3.56	3.54	3.56	3.52	
		PPL	34.98	35.10	34.41	35.24	33.64	
	dolma_common-crawl	Loss	3.23	3.23	3.22	3.23	3.20	
		PPL	25.32	25.25	25.09	25.35	24.55	
	dolma_pes2o	Loss	2.86	2.85	2.84	2.86	2.82	
		PPL	17.45	17.37	17.12	17.44	16.79	
	dolma_reddit	Loss	3.44	3.44	3.43	3.44	3.41	
		PPL	31.13	31.22	30.83	31.28	30.31	
	dolma_stack	Loss	1.42	1.41	1.40	1.42	1.39	
		PPL	4.13	4.09	4.07	4.13	4.02	
	dolma_wiki	Loss	3.04	3.03	3.03	3.04	3.00	
		PPL	20.89	20.78	20.61	20.88	20.10	
	ice	Loss	3.19	3.20	3.18	3.21	3.16	
		PPL	24.41	24.44	24.04	24.72	23.55	
	m2d2_s2orc	Loss	3.70	3.70	3.69	3.70	3.67	
		PPL	40.35	40.50	39.99	40.56	39.17	
	pile	Loss	2.74	2.73	2.72	2.74	2.70	
		PPL	15.44	15.39	15.17	15.50	14.87	
	wikitext_103	Loss	3.34	3.34	3.31	3.35	3.30	
		PPL	28.21	28.12	27.46	28.36	27.12	
	Average	Loss	3.07	3.06	3.05	3.07	3.03	
		PPL	24.28	24.28	23.94	24.39	23.47	
	Downstream Benchmarks	piqa	ACC	66.43	65.13	66.76	66.38	66.59
			ACC	33.87	33.96	34.22	33.92	35.15
hellaswag		ACC	52.80	51.62	50.12	51.07	51.38	
		ACC	28.00	28.00	28.80	28.60	28.40	
openbook_qa		ACC	70.30	70.90	70.40	70.20	70.30	
		ACC	45.44	48.60	47.02	44.91	48.95	
arc_easy		ACC	62.00	67.00	67.00	65.00	69.00	
		ACC	51.26	51.99	54.87	54.51	54.87	
commitment_bank		ACC	42.86	32.14	41.07	37.50	39.29	
		ACC	81.05	81.17	80.59	81.17	81.11	
mrpc		ACC	50.11	50.92	55.73	51.15	60.55	
		ACC	53.10	52.86	54.23	53.13	54.88	
sst2		ACC	53.10	52.86	54.23	53.13	54.88	
		ACC	53.10	52.86	54.23	53.13	54.88	
Average	ACC	53.10	52.86	54.23	53.13	54.88		

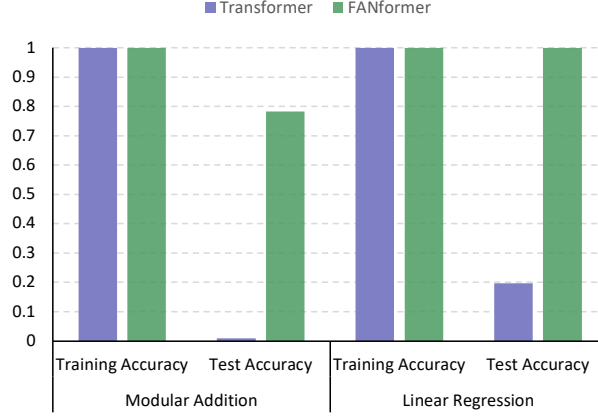
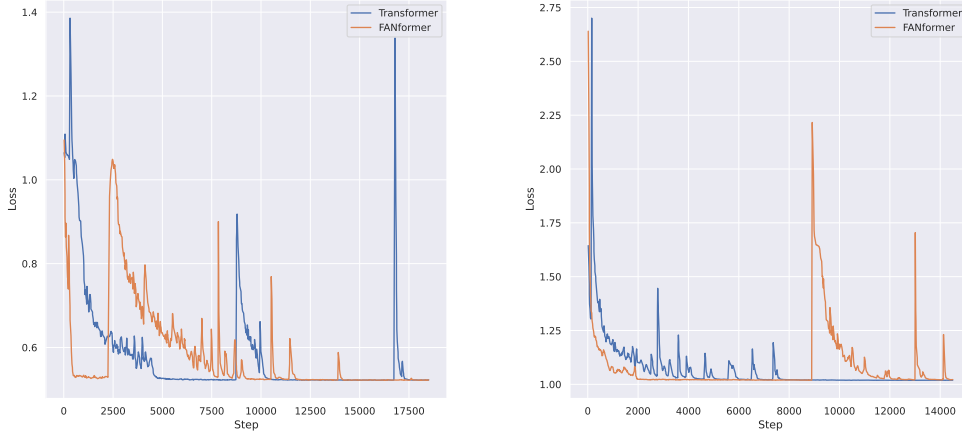


Figure 10: Training accuracy and test accuracy of FANformer and Transformer on modular addition and linear regression tasks.



(a) Training loss on modular addition task

(b) Training loss of linear regression task

Figure 11: Training loss of FAN and Transformer on case-based and rule-based reasoning.

K Case for Section 4.4.4

We present a case of FANformer and the baselines under a logical reasoning stress-test in Figure 13.

L Formal Proof of $\text{ATF}(\mathbf{X}) = \text{Attention}(\text{FANLayer}'(\mathbf{X}))$

Proposition 1. For an input sequence representation $\mathbf{X} \in \mathbb{R}^{n \times d}$, the ATF operator satisfies

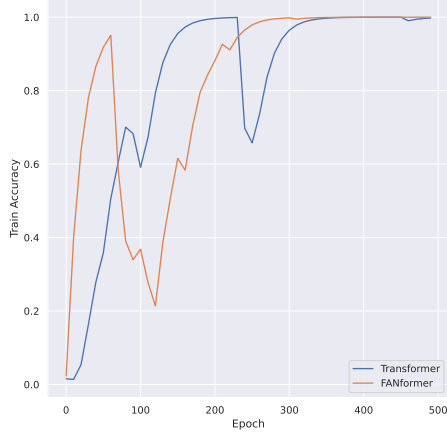
$$\text{ATF}(\mathbf{X}) = \text{Attention}(\text{FANLayer}'(\mathbf{X})).$$

Proof. By the definition of ATF via Eq. (3), we have

$$\text{ATF}(\mathbf{X}) = \text{softmax} \left(\frac{\mathbf{Q}_F \mathbf{K}_F^\top}{\sqrt{d_k}} \right) \mathbf{V}_F.$$

Substituting $\mathbf{Q}_F, \mathbf{K}_F, \mathbf{V}_F$ from Eq. (2) into Eq. (3) yields

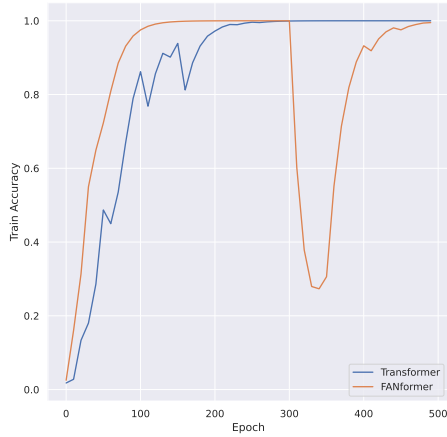
$$\text{ATF}(\mathbf{X}) = \text{softmax} \left(\frac{(\mathbf{X}_F \mathbf{W}_Q)(\mathbf{X}_F \mathbf{W}_K)^\top}{\sqrt{d_k}} \right) (\mathbf{X}_F \mathbf{W}_V)$$



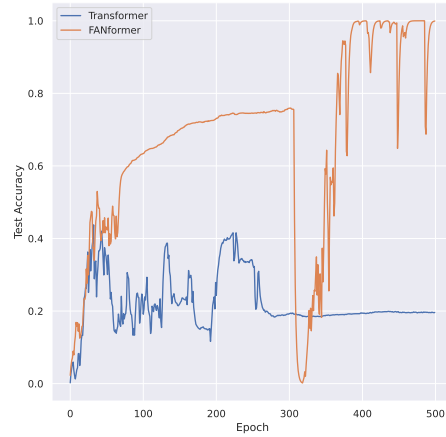
(a) Training accuracy on modular addition task



(b) Test accuracy of modular addition task



(c) Training accuracy on linear regression task



(d) Test accuracy of linear regression task

Figure 12: Accuracy of FAN and Transformer during training and testing on case-based and rule-based reasoning.

Matching to standard attention, for any input \mathbf{Z} , multi-head attention (single head shown for clarity) is defined as

$$\text{Attention}(\mathbf{Z}) = \text{softmax} \left(\frac{\mathbf{Z}\mathbf{W}_Q(\mathbf{Z}\mathbf{W}_K)^\top}{\sqrt{d_k}} \right) (\mathbf{Z}\mathbf{W}_V)$$

Thus, we have

$$\text{ATF}(\mathbf{X}) = \text{Attention}(\mathbf{X}_F). \quad (12)$$

Finally, substituting $\mathbf{X}_F = \text{FANLayer}'(\mathbf{X})$ via Eq. (1) into the above formula establishes the claim:

$$\text{ATF}(\mathbf{X}) = \text{Attention}(\text{FANLayer}'(\mathbf{X})).$$

□

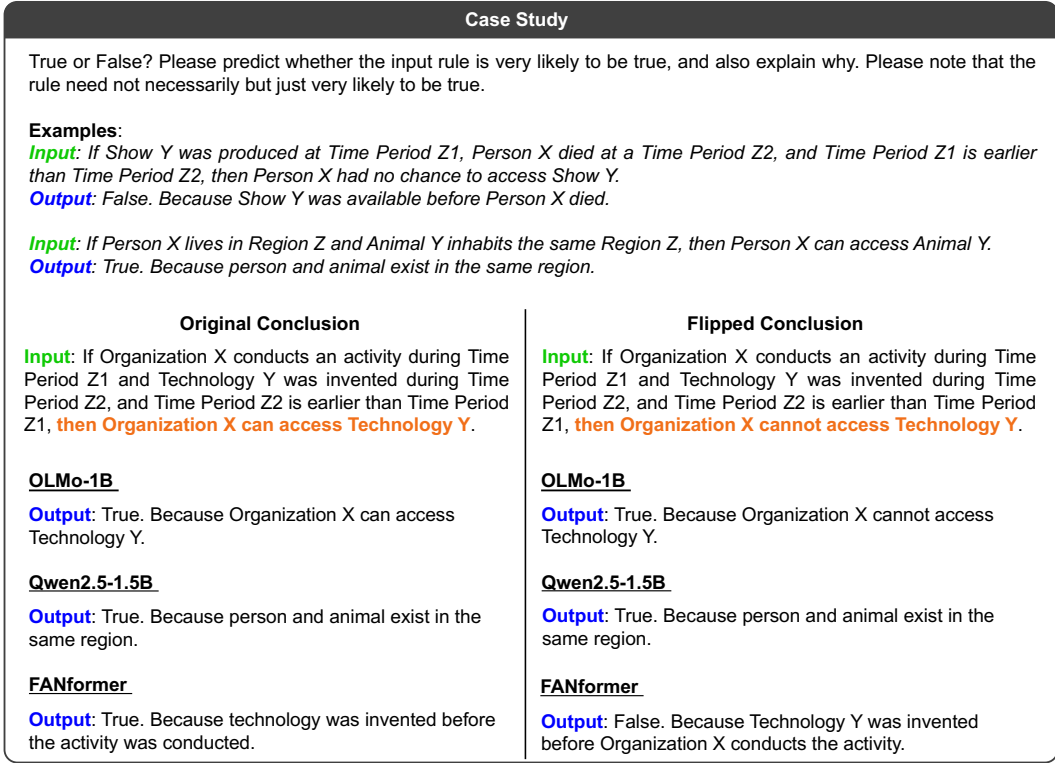


Figure 13: Case of FANformer and the baselines under logical reasoning stress-test.

M Comprehensive Experimental Details

M.1 Detailed training settings of FANformer

We train FANformer-1B using the ZeRO optimizer strategy [Rajbhandari et al., 2020] via PyTorch’s DDP framework [Li, 2018]. Following OLMo [Groeneveld et al., 2024], we use a constant global batch size of approximately 4M tokens (2048 instances, each with a sequence length of 2048 tokens). To improve throughput, we employ PyTorch’s amp module with the bfloat16 format. We employ the AdamW optimizer [Loshchilov and Hutter, 2019] for the model’s training process. The learning rate for all LLMs is set to 4.0e-4. We warm up the learning rate over 2000 steps (8B tokens) and then decay it in a cosine manner from there down to a tenth of the peak learning rate over the remainder of training. We employ FlashAttention [Dao et al., 2022] to accelerate the model training and inference processes, leveraging its ability to optimize memory usage and computational efficiency. The total GPU computational cost for pre-training FANformer-1B amounts to approximately 47,600 GPU hours.

M.2 Detailed Setup for Section 4.2

For different model sizes in Figure 3, the hidden dimension, number of layers, and number of heads are listed in Table 10.

M.3 Validation Set And Downstream Tasks

Following [Zhu et al., 2024], we use V2 Validation Sets, V3 Validation Sets, and Downstream tasks to evaluate our approach. The specific tasks included in V2 validation sets, V3 validation sets, and downstream tasks are listed in Table 11.

Table 10: Model size and setup used for FANformer in Section 4.2, where Transformers follows the setups of previous work OLMo [Groeneveld et al., 2024].

Model	Size	Hidden Dim.	Num Layers	Num Heads	Weight Tying
FANformer-300M	268M	1024	16	16	True
FANformer-600M	604M	1536	16	16	True
FANformer-1B	1.1B	2048	16	16	True
FANformer-3B	2.6B	2560	24	20	False
FANformer-7B	6.7B	4096	24	32	False

M.4 Detailed Setup of Case-based and Rule-based Reasoning.

Following the work [Hu et al., 2024], we focus on binary operations that take two numbers, a and b , as inputs. Denoting c as the target label, the constructed datasets are in the form of $\mathcal{D} = \{(a_i, b_i), c_i\}$ for two mathematical tasks: modular addition and linear regression. The two tasks are defined as follows:

- **Modular addition.** The input to the model is “ $a + b =$ ”, and the output is c , where $c = (a + b) \bmod P$. The values of a and b range from 0 to 112. The constant P is 113 here.
- **Linear regression.** This task involves the model learning a linear regression function. The input is given by “ $(a, b) =$ ”, and the output is c , where $c = m \cdot a + n \cdot b + p$. The values of a and b range from 0 to 99. The constants are set as $m = 1$, $n = 2$, and $p = 3$.

Leave-Square-Out The work [Hu et al., 2024] employs the Leave-Square-Out method to evaluate the generalization ability of the Transformer [Dong et al., 2024c]. In this approach, a square test set is created to isolate the test samples from the training samples. For instance, consider the center of the square at (a_k, b_k) with a side length of l_k . The square test set is defined as $\mathcal{T}_k = \{(a_i, b_i), c_i) \mid a_k - \frac{l_k}{2} \leq a_i \leq a_k + \frac{l_k}{2}, b_k - \frac{l_k}{2} \leq b_i \leq b_k + \frac{l_k}{2}\}$, and all remaining samples from the training set. This division creates a "hole" in the center of the training set, which is more challenging for the model compared to a random split. Since there are no similar cases in the training set to aid the model in solving the problem, this method tests whether the model has truly learned the underlying rules. In the experiments of the work [Hu et al., 2024], they found that Transformer-based models fail to generate correct answers for the test set in the "hole". Therefore, we use this method to assess the generalization ability of FANformer.

Settings We finetune both the Transformer and FANformer models on each dataset for 500 epochs. The batch size is set to 336, and the learning rate is initialized at 10^{-4} . A warm-up ratio of 0.01 is used, and we apply cosine decay to adjust the learning rate throughout the training process.

During generation, we set the model temperature to 0.5 and sample 10 generations to evaluate the accuracy on each test point. The square center (a_k, b_k) is (50, 50) for linear regression and (56, 56) for modular addition.

Following the work [Hu et al., 2024], we apply the Leave-Square-Out method to each dataset. Specifically, we extract a square comprising 441 samples (from a total of approximately 10,000 samples) with a side length of 20 to form our test set, leaving the remainder as the training set. It is important to note that, despite removing a small portion of training samples, we ensure that all tokens present in the dataset appear in the training set. This precaution is to prevent the models from failing simply due to encountering unseen tokens. We then proceed to finetune Transformer and FANformer models using this specific training-test split for each dataset.

M.5 Assessing LLMs’ Proficiency in Capturing Inferential Rules

Analysis Setup Following the experimental setup proposed by Wang et al. [2024], we adopt the ULogic framework to systematically evaluate LLMs on their ability to capture underlying inferential logic. Specifically, we leverage a curated probing subset comprising 1,104 diverse rules drawn from their rule base. These rules—manually verified by the original authors—span a range of lengths,

Table 11: Validation Set And Downstream Tasks.

V2 Validation Sets
v2-small-4chan-validation
v2-small-c4_100_domains-validation
v2-small-c4_en-validation
v2-small-gab-validation
v2-small-ice-validation
v2-small-m2d2_s2orc-validation
v2-small-m2d2_wiki-validation
v2-small-manosphere-validation
v2-small-mc4_en-validation
v2-small-pile-validation
v2-small-ptb-validation
v2-small-twitterAEE-validation
v2-small-wikitext_103-validation
V3 Validation Sets
v3-small-c4_en-validation
v3-small-dolma_books-validation
v3-small-dolma_common_crawl-validation
v3-small-dolma_pes2o-validation
v3-small-dolma_reddit-validation
v3-small-dolma_stack-validation
v3-small-dolma_wiki-validation
v3-small-ice-validation
v3-small-m2d2_s2orc-validation
v3-small-pile-validation
v3-small-wikitext_103-validation
Downstream Benchmarks
piqa [Bisk et al., 2020]
hellaswag [Zellers et al., 2019]
winogrande [Sakaguchi et al., 2020]
openbook_qa [Mihaylov et al., 2018]
sciq [Welbl et al., 2017]
arc_easy [Clark et al., 2018]
copa [Roemmele et al., 2011]
commitment_bank [De Marneffe et al., 2019]
mrpc [Dolan and Brockett, 2005]
rte [Dagan et al., 2005]
sst2 [Socher et al., 2013]

polarities, and structural patterns, ensuring broad coverage and high quality. The evaluation is framed as a binary entailment classification task, where the model must determine whether a given rule expresses a valid logical entailment. We employ a two-shot Chain-of-Thought (CoT) prompting method [Wei et al., 2022], in which each input includes one correct and one incorrect example to minimize label bias. The model is prompted not only to make a binary judgment but also to justify its reasoning, with an appended instruction such as "and also explain why."

To further enhance the reliability of the evaluation, we incorporate the Law of Non-Contradiction [Priest et al., 2006], which posits that statements of the form "If X, then Y" and "If X, then not Y" cannot simultaneously be true. Accordingly, for each original rule, we construct a flipped version by negating its conclusion. A rule is considered correctly classified only if the model affirms the original rule as true and rejects the flipped version as false, as illustrated below. We evaluate the base model of FANformer-1B, OLMo-1B, and Qwen2.5-1.5B, as well as GPT-4 on the two most challenging levels of ULogic for stress-testing (i.e., Length 3 and Length 4).

<i>If Premise, then Conclusion_{original}.</i>	True
<i>If Premise, then Conclusion_{flipped}.</i>	False

N Limitations

Our work has several limitations, which we aim to address in our future work:

First, due to constraints in computational resources, we only pretrain the FANformer-1B on 1 trillion tokens. However, our experimental results regarding FANformer’s scalability indicate that our FANformer demonstrates favorable scaling behavior during training, suggesting that increasing the model size and training tokens could lead to more significant performance improvements. To explore this further, we plan to seek additional computational resources to train larger-scale language models.

Second, our work is orthogonal to the existing approaches for revising the attention mechanism, i.e., our work can seamlessly incorporate them, as verified in the derivation provided in Appendix L. There are numerous variants of attention mechanisms, as discussed in the related work (Section 5), such as Flash Attention [Dao et al., 2022], MQA [Shazeer, 2019], and MLA [DeepSeek-AI et al., 2024b]. In this work, we only incorporate Flash Attention for necessary acceleration, while leaving the exploration of other approaches for future work.

Third, although we have observed that enhancing the ability of language models to model periodic patterns can improve language modeling performance, the underlying mechanisms responsible for this improvement remain underexplored. To the best of our knowledge, it has hardly been studied the role of periodicity or the potential periodic behaviors of LLMs on language modeling. Therefore, in future work, we will conduct a more comprehensive investigation into the fundamental mechanisms of periodicity in language modeling.